Journal of Solid Mechanics Vol. 14, No. 1 (2022) pp. 37-56
DOI: 10.22034/jsm.2020.1898465.1584

Improved High-Order Analysis of Linear Vibrations of a Thick Sandwich Panel with an Electro-Rheological Core by Using Exponential Shear Deformation Theory

M. Keshavarzian [1], M.M. Najafizadeh [1,*], K. Khorshidi [2], P. Yousefi [1], M.Alavi [3]

[1]*Department of Mechanical Engineering, Arak Branch, Islamic Azad University, Arak, Iran*
[2]*Department of Mechanical Engineering, Faculty of Engineering, Arak University, Arak, Iran*
[3]*Department of Mathematics, Arak branch, Islamic Azad University, Arak, Iran*

Received 4 September 2021; accepted 8 December 2021

ABSTRACT
In this paper, the behavior of free vibrations of the thick sandwich panel with multi-layer face sheets and an electrorheological (ER) fluid core using Exponential Shear Deformation Theory were investigated. For the first time, Exponential shear deformation theory is used for the face sheets while the Displacement field based on the second Frostig's model is used for the core. The governing equations and the boundary conditions are derived by Hamilton's principle. Closed form solution is achieved using the Navier method and solving the eigenvalues. Primary attention is focused on the effects of electric field magnitude, geometric aspect ratio, and ER core layer thickness on the dynamic characteristics of the sandwich plate. The rheological property of an ER material, such as viscosity, plasticity, and elasticity may be changed when applying an electric field. When an electric field is applied, the damping of the system is more effective. The effects of the natural frequencies and loss factors on the dynamic behavior of the sandwich plate are studied. The natural frequency of the sandwich plate increases and the modal loss factor decreases. With increasing the thickness of the ER layer, the natural frequencies of the sandwich plate are decreased.

Keywords: Sandwich plate; Electro-rheological materials; Electric field; Exponential shear deformation theory; Free vibration.

1 INTRODUCTION

MAGNETORHEOLOGICAL (MR) and electrorheological (ER) materials belong to a family of controllable fluids. Their rheological properties such as viscosity, elasticity and plasticity change in the order of milliseconds in response to applied magnetic and electric field levels, respectively. ER materials are electrical analogs of MR materials. They are dielectric particles suspended in non-polar liquids. Their reversible rheological behavior is controlled by electrical field strength. Both MR and ER fluids are in liquid form when there is no

[*]Corresponding author. Tel.: +98 86 34134025; Fax.: +98 86 34134025.
E-mail address: m-najafizadeh@iau-arak.ac.ir (M.M.Najafizadeh)

external stimuli. However, when they are subjected to an applied magnetic field (for MR materials) and an electric field (for ER materials), their physical appearance changes to be more like a solid gel. As described earlier, during this transformation, their rheological properties change as well. Fig. 1 is a schematic drawing of stress–strain behavior of ER and MR materials for a varying range of electric and magnetic fields. Although MR and ER materials experience different levels of stress and strain in response to different magnetic and electric fields respectively, they follow the same type of pattern in their rheological behavior. The ER and MR materials are used in adaptive structures to produce variable dynamic response characteristics such as natural frequencies, mode shapes and vibration amplitudes. The yield stress depends on the electric field applied to the liquid, but we reach a point where the magnification of the electric field does not increase further, and the liquid at this point becomes magnetically saturated. Therefore, the fluid behavior of ER can be assumed to be the same as the Bingham plastic model, a model that is being further investigated. Therefore, there is no normal stress in the ER layer [1].

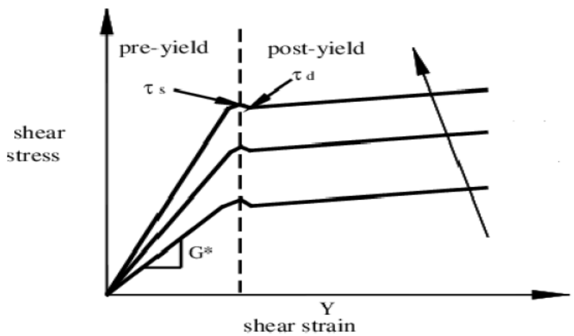

Fig.1
Shear stress–shear strain relationship of ER and MR materials.

To suppress such vibrations two approaches can be used, namely, passive control and active control. In passive control the material properties of the structure itself, such as damping and stiffness, are modified so as to change the structural response. However, the material properties of such structures are predetermined in their design or construction phase, and can be hardly adapted to unexpected environmental changes. In order to overcome this disadvantage, intelligent materials such as piezoelectric materials or electrorheological fluids (ERFs) may be incorporated into conventional structures in order to adapt to changes of the environment [2]. Early investigations of an ER material in the structural vibration control problems can be traced to Coulter and coworkers [3-5], who performed theoretical and experimental studies of flexural vibrations of ER fluid-based sandwich beams by applying variable electric field levels to the ER material. Yalcintas and Coulter [6, 7] presented a study on the modeling and (semi-active) vibration control problem of an adaptive sandwich beam with an ER fluid core treatment as a controllable damping layer. Yeh and Chen Wang, studied the dynamic stability problems of the ER sandwich beam and also discussed the dynamic behavior of the sandwich plate (annular plate, orthotropic sandwich plates, orthotropic annular plate, and rotating polar orthotropic annular plate) on different thickness of the ER layer and electric filed strength [8-13]. The higher order sandwich panel theory was developed by Frostig et al. [14], who considered two types of computational models in order to express governing equations of the core layer. The second model assumed a polynomial description of the displacement fields in the core that was based on displacement fields of the first model. He uses the classical thin plate theory for the face sheets. In the higher-order sandwich panel theory (the second Frostig's model) The transverse normal stress in the face sheets and the in-plane stresses in the core were not considered. An improved high-order theory is presented to investigate the dynamic behavior of thin and thick plate with a soft viscoelastic flexible core. Shear deformation theory is used for the face sheets while three-dimensional elasticity theory is used for the soft core. In this theory transverse shear and rotary inertia effects of face sheets and all stress components are taken into consideration [15]. The improved higher order sandwich plate theory (IHSAPT), applying the first-order shear deformation theory for the face sheets, was introduced by Malekzadeh et al. [15]. First order shear deformation theory [16,17] incorporates the shear deformation effects but it considers a constant transverse shear deformation along thickness of plate. Thus, it violates stress free conditions at the bottom and top of the plate and needs a shear correction factor. In order to get accurate results and avoiding to use of shear correction factor, higher order shear deformation theory (HSDT) developed. Reddy [16] employed a parabolic shear stress distribution along thickness of plate. his model didn't need shear correction factor because of satisfying free stress conditions at the bottom and top of plate. The mechanical behavior of sheets is often studied and analyzed using plate theories. Most plate and shell theories are based on a kinematic assumption of displacement or the deformation of the object in three dimensions. Sayyad and Ghugal [20] presented exponential and trigonometric shear deformation theories for bending and free vibration analysis of thick plates. Bending analysis of composite sandwich plates with laminated face sheets with new finite element formulation has been done by Belarbi and Tati [19]. Free vibration of functionally graded rectangular nanoplates has been studied by Khorshidi and Asgari [20]. They used exponential shear deformation theory in their analysis. Bahrami and Hatami [21] studied free and forced transverse vibration analysis of moderately thick orthotropic plates using spectral finite element method. Mozaffari et al. [22] examined the memory alloys on the free vibration behavior of flexible-core sandwich-composite panels. Ghajar et al. [23] also analyzed the dynamic response of the double-curved composite shell under low velocity impact. Khorshidi et al. [24] investigated the electro-mechanical free vibrations analysis of composite rectangular piezoelectric nanoplate using modified shear deformation theories. Ghorbanpour Arani et al. [25] investigated the analysis of viscoelastic functionally graded sandwich plates with CNT reinforced composite face sheets on viscoelastic foundation. One of the most important damages of sandwich structures is the separation in the middle layer between the core and the Shell. The reason for this separation is the difference of the Young's modulus ratio between the core and the face sheet. Use of a material with high shear stress tolerance in the core will weaken the adhesion of the middle layer. The core use of FGM or ER smart fluids eliminates all of these problems. Under the influence of electric fields, intelligent fluids exhibit rapid changes in hardness and damping properties. These fluids are also very suitable for vibration control over very large ranges. The concept of material-based ER adaptive structures was first put forward by Carlson et al. [26]. Most of the work published in the last few years has focused mainly on the experimental and theoretical aspects of ER adaptive structures [27-6]. Free vibration and buckling analysis of sandwich panels with flexible cores using an improved higher order theory has been studied by Malekzadeh Fard and Malek-Mohammadi [28]. However, research on adaptive MR sandwich structures is in its infancy. Some research has investigated the vibrational and damping properties of ER and MR materials with adaptive structures [29-30]. Yeh et al. [12] examined the vibrational properties and modal damping coefficient of circular sandwich sheets with orthotropic face sheet and ER core. Ramkomar and Gensan [31] used ER fluids as the core of a sandwich hollow column wall and compared the performance of ER fluid application with viscoelastic materials in changing the vibrational properties of the column. The most recent work on MR fluids is the work of Rajamohan et al. [32]. They modeled a sandwich beam with an MR core, considering the shear effects of the MR binding layer on the core and applying the equivalent shear modulus. They applied the finite element method to solve the problem and investigated the effects of magnetic field intensity on vibrational properties for different boundary conditions and forced loading. Rajamohan et al. [33] also for the first time investigated the vibrational properties of a partially filled MR sandwich beam both via the finite element method and experimentally. Rajamohan et al. [34] also for the first time explored the model presented in reference [33] to find the optimal location of partial MR layers for maximizing the modal damping coefficient of sandwich beams. They tested the optimal location of the partial MR layers to maximize the first five modal damping coefficients of the beam separately and simultaneously. Free vibration of sandwich panels with smart magneto-rheological layers and flexible cores has been studied by Payganeh et al. [35].

In this study, based on the displacement field of each layer, the kinetic energy and strain energy are separately obtained for each layer. With the replacement of total kinetic energy, total strain energy and energy variations, in the Hamiltonian principle, the structural motion equation is obtained. Primary attention is focused on the effects of electric field magnitude, geometric aspect ratio, and ER core layer thickness on the dynamic characteristics of the sandwich plate. Natural frequencies and loss factor for the electric fields as well as the ratio of different thicknesses calculated are by Galerkin analytical method. As the applied electric field increases, the natural frequency of the sandwich plate increases and the modal loss factor decreases. With increasing the thickness of the ER layer, the natural frequencies of the sandwich plate are decreased.

2 THEORETICAL FORMULATION

The assumptions intended for modeling the problem are as follows:

Face sheets are elastic and can be isotropic , orthotropic, or composite material. It is assumed that there is no slip between the elastic layers of the ER layer. Transverse displacement is assumed to be identical for all points on a hypothetical cross-sectional area. It is assumed that there is no normal stress in the ER layer. The ER is modeled as a linear viscoelastic material in pre-submission conditions. The ER used in the core completely covers the core with the displacements considered linear and small, and the face sheet are assumed as thin. Fig. 2 shows a flat sandwich sheet with two laminated composite sheets on its faces. The thickness of the top sheet, the bottom sheet and the core are as follows h_t, h_b, h_c . The sandwich panel is supposed to have length *a*, width *b* and total thickness *h*. The orthogonal coordinates $(x_i, y_i, z_i \quad i = t, b, c)$ are also shown in Fig. 1. In this study, the *t* index corresponds to the upper sheet, the *b* index to the lower sheet, and the *c* index to the core.

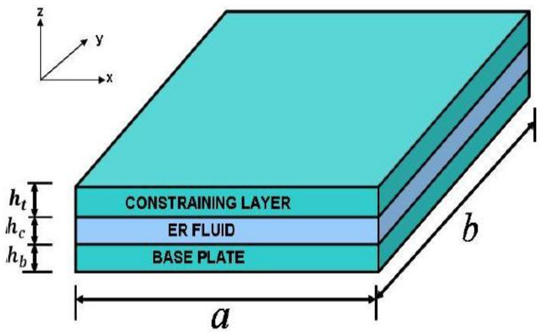

Fig.2
Sandwich plate with laminated composite sheets on the surfaces.

2.1 Displacement fields and strain relations displacement for face sheets and cores

According to the exponential shear deformation theory, the displacements *u, v*, and *w* face sheets in the *x, y* and *z* directions assuming small linear displacements as Eqs. (1):

$$\begin{aligned}
u_i(x,z,y,t) &= u_0^i(x,y,t) - z_i \frac{\partial w_0^i(x,y,t)}{\partial x} + z_i e^{-2\left(\frac{z_i}{h}\right)^2} \phi_x^i(x,y,t) \\
v_i(x,z,y,t) &= v_0^i(x,y,t) - z_i \frac{\partial w_0^i(x,y,t)}{\partial x} + z_i e^{-2\left(\frac{z_i}{h}\right)^2} \phi_y^i(x,y,t) \\
w_i(x,z,y,t) &= w_0^i(x,y,t); \qquad (i = t,b)
\end{aligned} \tag{1}$$

where z_i is vertical coordinate of the each face sheet $(i = t, b)$, measured upward from the mid-plane of each face sheet. Kinematic equations of the face sheets are as follows:

$$\begin{aligned}
&\varepsilon_{xx}^i = \varepsilon_{0xx}^i - z_i L_{xx}^i + z_i e^{-2\left(\frac{z_i}{h}\right)^2} k_{xx}^i, \qquad \varepsilon_{yy}^i = \varepsilon_{0yy}^i - z_i L_{yy}^i + z_i e^{-2\left(\frac{z_i}{h}\right)^2} k_{yy}^i, \qquad \varepsilon_{zz}^i = 0 \\
&\gamma_{xy}^i = 2\varepsilon_{xy}^i = \varepsilon_{0xy}^i - z_i L_{xz}^i + z_i e^{-2\left(\frac{z_i}{h}\right)^2} k_{xy}^i, \qquad i = t,b \\
&\gamma_{xz}^i = 2\varepsilon_{xz}^i = \varepsilon_{0xz}^i - G_{xz}^i + e^{-2\left(\frac{z_i}{h}\right)^2} \left[1 - 4\left(\frac{z_i}{h}\right)^2\right] T_{xz}^i, \qquad \gamma_{yz}^i = 2\varepsilon_{yz}^i = \varepsilon_{0yz}^i - G_{yz}^i + e^{-2\left(\frac{z_i}{h}\right)^2} [1 - 4\left(\frac{z_i}{h}\right)^2]\, T_{yz}^i
\end{aligned} \tag{2}$$

$$\begin{aligned}
&\varepsilon_{0xx}^i = \frac{\partial u_0^i}{\partial x}, \quad L_{xx}^i = \frac{\partial^2 w_0^i}{\partial x^2}, \quad K_{xx}^i = \frac{\partial \phi_x^i}{\partial x}, \quad \varepsilon_{0yy}^i = \frac{\partial v_0^i}{\partial y}, \quad L_{yy}^i = \frac{\partial^2 w_0^i}{\partial y^2}, \quad K_{yy}^i = \frac{\partial \phi_y^i}{\partial y}, \\
&\varepsilon_{0xy}^i = \frac{\partial v_0^i}{\partial x} + \frac{\partial u_0^i}{\partial y}, \quad L_{xy}^i = \frac{2\partial^2 w_0^i}{\partial y\, \partial x}, \quad K_{xy}^i = \frac{\partial \phi_y^i}{\partial x} + \frac{\partial \phi_x^i}{\partial y}, \\
&\varepsilon_{0xz}^i = \frac{\partial w_0^i}{\partial x}, \quad G_{xz}^i = \frac{\partial w_0^i}{\partial x}, \quad T_{xz}^i = \phi_x^i, \quad \varepsilon_{0yz}^i = \frac{\partial w_0^i}{\partial y}, \quad G_{yz}^i = \frac{\partial w_0^i}{\partial y}, \quad T_{yz}^i = \phi_y^i
\end{aligned} \tag{3}$$

As can be seen, ε_{zz} for the face sheets is equal to zero. This means that the face sheets are assumed to be rigid in the *Z* direction. Displacement relations are based on Frostig's second model for the thick core in the form of a relation (4) [14]:

$$\begin{cases} u_c(x,y,z,t) = u_0^c(x,y,t) + z_c u_1^c(x,y,t) + z_c^2 u_2^c(x,y,t) + z_c^3 u_3^c(x,y,t) \\ v_c(x,y,z,t) = v_0^c(x,y,t) + z_c v_1^c(x,y,t) + z_c^2 v_2^c(x,y,t) + z_c^3 v_3^c(x,y,t) \\ w_c(x,y,z,t) = w_0^c(x,y,t) + z_c w_1^c(x,y,t) + z_c^2 w_2^c(x,y,t) \end{cases} \tag{4}$$

The kinematic relationships of the core in a sandwich sheet are based on the relation of small deformations (5):

$$\begin{aligned} &\varepsilon_{xx}^c = \left(\frac{\partial u_c}{\partial x}\right), \qquad \varepsilon_{yy}^c = \left(\frac{\partial v_c}{\partial y}\right), \qquad \varepsilon_{zz}^c = w_1^c + 2zw_2^c, \\ &\gamma_{xy}^c = 2\varepsilon_{xy}^c = \frac{\partial v_c}{\partial x} + \frac{\partial u_c}{\partial y}, \qquad \gamma_{xz}^c = 2\varepsilon_{xz}^c = \left(\frac{\partial w_c}{\partial x}\right) + \frac{\partial u_c}{\partial z}, \qquad \gamma_{yz}^c = 2\varepsilon_{yz}^c = \left(\frac{\partial w_c}{\partial y}\right) + \frac{\partial v_c}{\partial z} \end{aligned} \tag{5}$$

2.2 Compatibility cnditions

The research assumes that the face sheets are ideally attached to the core. In other words, there is a displacement continuity in the subscriber season. Thus, all three components of the upper-case and core displacements are equal in the common season. This is also the case for the low-core joint face sheet chapter. Thus, assuming complete bending between the core and the surfaces, the compatibility conditions for the top and bottom joining of the core and the surfaces are as follows:

$$\begin{aligned} &u_c(z = z_{ci}) = u_0^i + \frac{1}{2}(-1)^k\, h_i \phi_x^i, \\ &v_c(z = z_{ci}) = v_0^i + \frac{1}{2}(-1)^k\, h_i \phi_y^i, \\ &w_c(z = z_{ci}) = w_0^i \\ &i = t \to k = 1; z_{ct} = \frac{h_c}{2}, \qquad i = b \to k = 0;\; z_{cb} = -\frac{h_c}{2}, \end{aligned} \tag{6}$$

By replacing Eqs. (4) and (6) in relation (5) and some simplification, the compatibility conditions are transformed into (7):

$$\begin{aligned} &u_2^c = \frac{\left[2\left(u_0^t + u_0^b\right) - h_t\phi_x^t + h_b\phi_x^b - 4u_0^c\right]}{h_c^2}, \qquad u_3^c = \frac{\left[4\left(u_0^t + u_0^b\right) - 2\left(h_t\phi_x^t + h_b\phi_x^b\right) - 4h_c u_1^c - 4h_c u_0^c / R_{xc}\right]}{h_c^3} \\ &v_2^c = \frac{\left[2\left(v_0^t + v_0^b\right) - h_t\phi_y^t + h_b\phi_y^b - 4v_0^c\right]}{h_c^2}, \qquad v_3^c = \frac{\left[4\left(v_0^t + v_0^b\right) - 2\left(h_t\phi_y^t + h_b\phi_y^b\right) - 4h_c v_1^c - 4h_c v_0^c / R_{yc}\right]}{h_c^3} \\ &w_1^c = \frac{\left[2\left(w_0^t + w_0^b\right)\right]}{h_c^2}, \qquad w_2^c = \frac{\left[2\left(w_0^t + w_0^b\right) - 4w_0^c\right]}{h_c^2} \end{aligned} \tag{7}$$

According to Eq. (7), it is observed that the number of unknowns in the core layer is reduced to five, which are: $u_1^c, u_0^c, v_0^c, v_1^c, w_0^c$. Thus, in general, all the unknowns for a flat composite sandwich sheet are 15, which are [36]:

$$\{u_0^t, v_0^t, w_0^t, \psi_x^t, \psi_y^t, u_0^b, v_0^b, w_0^b, \psi_x^b, \psi_y^b, u_0^c, u_1^c, v_0^c, v_1^c, w_0^c\} \tag{8}$$

2.3 Relationships of stresses, resulting stresses, and moments of inertia in the core and face sheet

Based on the existing information on the ER material pre-yield rheology, only the electric field dependence of ER material in the pre-yield regime needs to be considered. The complex modulus of the used ER fluid was experimentally measured by Don [27] and can be expressed as follows:

$$G^{C}_{2a(xz)}=G'^{C}_{2a(xz)}+iG''^{C}_{2a(xz)},\quad G^{C}_{2a(yz)}=G'^{C}_{2a(yz)}+iG''^{C}_{2a(yz)}$$
$$G'^{C}_{2a(xz)}=G'^{C}_{2a(yz)}=15000E^{2},\quad G''^{C}_{2a(xz)}=G''^{C}_{2a(yz)}=6900 \tag{9}$$

where G'^{C}_{a} is the shear storage modulus and G''^{C}_{a} is the loss modulus and E is the electric field in *kV/mm*. In the following discussions, another modified ER material presented by Yalcintas [6] is also investigated in this study. The modified material properties of the ER fluid is:

$$G^{C}_{2b(xz)}=G'^{C}_{2b(xz)}+iG''^{C}_{2b(xz)},\quad G^{C}_{2b(yz)}=G'^{C}_{2b(yz)}+iG''^{C}_{2b(yz)}$$
$$G'^{C}_{2b(xz)}=G'^{C}_{2b(yz)}=50000E^{2},\quad G''^{C}_{2b(xz)}=G''^{C}_{2b(yz)}=2600E+1700 \tag{10}$$

where $G'^{C}_{b(xz)}$, $G'^{C}_{b(yz)}$ the shear storage modulus and $G''^{C}_{b(xz)}$, $G''^{C}_{b(yz)}$ is the loss modulus, and E is the electric field in *kV/mm*. As mentioned, there is no normal stress in the ER layer and only transverse shear stresses are:

$$\sigma^{c}_{xz}=G^{C}_{2b(xz)}\gamma^{C}_{xz}=G^{C}_{2b(xz)}\left[w^{C}_{0,x}+zw^{C}_{1,x}+z^{2}w^{C}_{2,x}\right]+G^{C}_{2b(xz)}\left[u^{C}_{1}+2zu^{C}_{2}+3z^{2}u^{C}_{3}\right]$$
$$\sigma^{c}_{yz}=G^{C}_{2b(yz)}\gamma^{C}_{yz}=G^{C}_{2b(yz)}\left[w^{C}_{0,y}+zw^{C}_{1,y}+z^{2}w^{C}_{2,y}\right]+G^{C}_{2b(yz)}\left[v^{C}_{1}+2zv^{C}_{2}+3z^{2}v^{C}_{3}\right] \tag{11}$$

The effect of the electric field on the vibration response of the ER sandwich plate can be seen for electric field levels of 0.5 , 1.5 , 2 , and 3.5 *kV/mm*, respectively. The results of the stress for the core can be written as follows [37]:

$$\begin{Bmatrix}N^{C}_{xx}\\N^{C}_{yy}\\N^{C}_{xy}\end{Bmatrix}=\int_{-h_c/2}^{h_c/2}\begin{Bmatrix}\sigma^{C}_{xx}\\\sigma^{C}_{yy}\\\sigma^{C}_{xy}\end{Bmatrix}dz_c,\quad \begin{Bmatrix}M^{C}_{nxx}\\M^{C}_{nyy}\\M^{C}_{nxy}\end{Bmatrix}=\int_{-h_c/2}^{h_c/2}z_c^{n}\begin{Bmatrix}\sigma^{C}_{xx}\\\sigma^{C}_{yy}\\\sigma^{C}_{xy}\end{Bmatrix}dz_c,\quad \begin{Bmatrix}N^{C}_{xz}\\N^{C}_{yz}\\M^{C}_{nxz}\\M^{C}_{nyz}\end{Bmatrix}=\int_{-h_c/2}^{h_c/2}z_c^{n}\begin{Bmatrix}\sigma^{C}_{xz}\\\sigma^{C}_{yz}\\z_c^{n}\sigma^{C}_{xz}\\z_c^{n}\sigma^{C}_{yz}\end{Bmatrix}dz_c,$$
$$\left\{R^{C}_{z},M^{C}_{z}\right\}=\int_{-h_c/2}^{h_c/2}\left(1,z_c\right)\sigma^{C}_{zz}dz_c,\qquad n=1,2,3 \tag{12}$$

Stress resultants per unit length for the face sheets can be defined as follows:

$$\begin{Bmatrix}N^{i}_{xx}\\N^{i}_{yy}\\N^{i}_{xy}\end{Bmatrix}=\int_{-h_i/2}^{h_i/2}\begin{Bmatrix}\sigma^{i}_{xx}\\\sigma^{i}_{yy}\\\sigma^{i}_{xy}\end{Bmatrix}dz_i,\quad \begin{Bmatrix}M^{i}_{xx}\\M^{i}_{yy}\\M^{i}_{xy}\end{Bmatrix}=\int_{-h_i/2}^{h_i/2}z_i\begin{Bmatrix}\sigma^{i}_{xx}\\\sigma^{i}_{yy}\\\sigma^{i}_{xy}\end{Bmatrix}dz_i,\quad \begin{Bmatrix}P^{i}_{xx}\\P^{i}_{yy}\\P^{i}_{xy}\end{Bmatrix}=\int_{-h_i/2}^{h_i/2}z_i e^{-2\left(\frac{z_i}{h}\right)^{2}}\begin{Bmatrix}\sigma^{i}_{xx}\\\sigma^{i}_{yy}\\\sigma^{i}_{xy}\end{Bmatrix}dz_i,$$
$$N^{i}_{xz}=k_s\int_{-h_i/2}^{h_i/2}\sigma^{i}_{xz}dz_i,\quad R^{i}_{xz}=k_s\int_{-h_i/2}^{h_i/2}z_i\sigma^{i}_{xz}dz_i,\quad S^{i}_{xz}=k_s\int_{-h_i/2}^{h_i/2}e^{-2\left(\frac{z_i}{h}\right)^{2}}\left[1-4\left(\frac{z_i}{h}\right)^{2}\right]\sigma^{i}_{xz}dz_i,\quad i=t,b$$
$$N^{i}_{yz}=k_s\int_{-h_i/2}^{h_i/2}\sigma^{i}_{yz}dz_i,\quad R^{i}_{yz}=k_s\int_{-h_i/2}^{h_i/2}z_i\sigma^{i}_{yz}dz_i,\quad S^{i}_{yz}=k_s\int_{-h_i/2}^{h_i/2}e^{-2\left(\frac{z_i}{h}\right)^{2}}\left[1-4\left(\frac{z_i}{h}\right)^{2}\right]\sigma^{i}_{yz}dz_i,\quad i=t,b \tag{13}$$

where k_s is Shear correction factor and $f_1(z_i),f_2(z_i)$ denotes $z_i, z_i e^{2\left(\frac{z_i}{h}\right)^{2}}$ respectively.

2.4 Lamina constitutive relations

The linear constitutive Relations for *kth* orthotropic Lamina in the principle material coordinates of a lamina are:

$$\begin{bmatrix}\sigma_{xx}\\ \sigma_{yy}\\ \sigma_{xy}\end{bmatrix}=\begin{bmatrix}Q_{11} & Q_{12} & Q_{16}\\ Q_{12} & Q_{22} & Q_{26}\\ Q_{16} & Q_{26} & Q_{66}\end{bmatrix}^{(k)}\begin{bmatrix}\varepsilon_{xx}\\ \varepsilon_{yy}\\ \varepsilon_{xy}\end{bmatrix},\qquad \begin{bmatrix}\sigma_{yz}\\ \sigma_{xz}\end{bmatrix}=\begin{bmatrix}Q_{44} & Q_{45}\\ Q_{45} & Q_{55}\end{bmatrix}^{(k)}\begin{bmatrix}\varepsilon_{yz}\\ \varepsilon_{xz}\end{bmatrix} \tag{14}$$

where $Q_{ij}^{(k)}$ are the plane stress-reduced stiffnesses. The coefficient $Q_{ij}^{(k)}$ are known in terms of the engineering constants of the *kth* layer:

$$Q_{11}=\frac{E_1}{1-v_{12}v_{21}},\ \ Q_{12}=\frac{v_{12}E_1}{1-v_{12}v_{21}},\ \ Q_{22}=\frac{E_2}{1-v_{12}v_{21}},\ \ Q_{66}=G_{12},\ \ Q_{44}=G_{23},\ \ Q_{55}=G_{13} \tag{15}$$

Since the laminate is made of several orthotropic layers, with their material axes oriented arbitrarily with respect to the laminate coordinates, the constitutive equations of each layer must be transformed to the laminates coordinates. The stress- strain relations in the direction of the sandwich panel geometrical axes as follows:

$$\begin{bmatrix}\sigma_{xx}\\ \sigma_{yy}\\ \sigma_{xy}\end{bmatrix}=\begin{bmatrix}\bar{Q}_{11} & \bar{Q}_{12} & \bar{Q}_{16}\\ \bar{Q}_{12} & \bar{Q}_{22} & \bar{Q}_{26}\\ \bar{Q}_{16} & \bar{Q}_{26} & \bar{Q}_{66}\end{bmatrix}^{(k)}\begin{bmatrix}\varepsilon_{xx}\\ \varepsilon_{yy}\\ \varepsilon_{xy}\end{bmatrix},\qquad \begin{bmatrix}\sigma_{yz}\\ \sigma_{xz}\end{bmatrix}=\begin{bmatrix}\bar{Q}_{44} & \bar{Q}_{45}\\ \bar{Q}_{45} & \bar{Q}_{55}\end{bmatrix}^{(k)}\begin{bmatrix}\varepsilon_{yz}\\ \varepsilon_{xz}\end{bmatrix} \tag{16}$$

where $\bar{Q}_{ij}$ denotes the transmitted stiffness in the geometric axis of the sandwich panel. The relationship between axial stiffness and the transferred stiffness is given by the relation:

$$\begin{aligned}
\bar{Q}_{11}&=Q_{11}\cos^4\theta+2\left(Q_{12}+2Q_{66}\right)\sin^2\theta\cos^2\theta+Q_{22}\sin^4\theta\\
\bar{Q}_{12}&=\left(Q_{11}+Q_{22}-4Q_{66}\right)\sin^2\theta\cos^2\theta+Q_{12}\left(\sin^4\theta+\cos^4\theta\right)\\
\bar{Q}_{22}&=Q_{11}\sin^4\theta+2\left(Q_{12}+2Q_{66}\right)\sin^2\theta\cos^2\theta+Q_{22}\cos^4\theta\\
\bar{Q}_{16}&=\left(Q_{11}-Q_{12}-2Q_{66}\right)\sin\theta\cos^3\theta+\left(Q_{12}-Q_{22}+2Q_{66}\right)\sin^3\theta\cos\theta\\
\bar{Q}_{26}&=\left(Q_{11}-Q_{12}-2Q_{66}\right)\sin^3\theta\cos\theta+\left(Q_{12}-Q_{22}+2Q_{66}\right)\sin\theta\cos^3\theta\\
\bar{Q}_{66}&=\left(Q_{11}+Q_{22}-2Q_{12}-2Q_{66}\right)\sin^2\theta\cos^2\theta+Q_{66}\left(\sin^4\theta\cos^4\theta\right)\\
\bar{Q}_{44}&=Q_{44}\cos^4\theta+Q_{55}\sin^4\theta\\
\bar{Q}_{45}&=\left(Q_{55}-Q_{44}\right)\cos\theta\sin\theta\\
\bar{Q}_{55}&=Q_{55}\cos^4\theta+Q_{44}\sin^4\theta
\end{aligned} \tag{17}$$

The basic multi-layer relationships of the face sheet are derived from the following relationship:

$$\begin{aligned}
N^i_{xx}&=A^i_{11}(\frac{\partial u_0^i}{\partial x})+B^i_{11}(\frac{\partial^2 w_0^i}{\partial x^2})+D^i_{11}\frac{\partial\phi_x^i}{\partial x}+A^i_{12}\frac{\partial v_0^i}{\partial y}+B^i_{12}\frac{\partial^2 w_0^i}{\partial y^2}+D^i_{12}\frac{\partial\phi_y^i}{\partial y}+A^i_{16}(\frac{\partial u_0^i}{\partial y}+\frac{\partial v_0^i}{\partial x})+\\
&B^i_{16}(2\frac{\partial^2 W_0^i}{\partial x\,\partial y})+D^i_{16}(\frac{\partial\phi_x^i}{\partial y}+\frac{\partial\phi_y^i}{\partial x})\\
N^i_{yy}&=A^i_{12}(\frac{\partial u_0^i}{\partial x})+B^i_{12}\frac{\partial^2 w_0^i}{\partial x^2}+D^i_{12}\frac{\partial\phi_x^i}{\partial x}+A^i_{22}(\frac{\partial v_0^i}{\partial y})+B^i_{22}(\frac{\partial^2 w_0^i}{\partial y^2})+D^i_{22}(\frac{\partial\phi_y^i}{\partial y})+A^i_{26}(\frac{\partial u_0^i}{\partial y}+\frac{\partial v_0^i}{\partial x})\\
&+B^i_{26}(2\frac{\partial^2 W_0^i}{\partial x\,\partial y})+D^i_{26}(\frac{\partial\phi_x^i}{\partial y}+\frac{\partial\phi_y^i}{\partial x})
\end{aligned} \tag{18}$$

$$N^i_{xy} = A^i_{16}(\frac{\partial u_0^i}{\partial x}) + B^i_{16}(\frac{\partial^2 w_0^i}{\partial x^2}) + D^i_{16}\frac{\partial \phi_x^i}{\partial x} + A^i_{26}\frac{\partial v_0^i}{\partial y} + B^i_{26}\frac{\partial^2 w_0^i}{\partial y^2} + D^i_{26}\frac{\partial \phi_y^i}{\partial y} + A^i_{66}(\frac{\partial u_0^i}{\partial y} + \frac{\partial v_0^i}{\partial x})$$
$$+B^i_{66}(2\frac{\partial^2 W_0^i}{\partial x\,\partial y}) + D^i_{66}(\frac{\partial \phi_x^i}{\partial y} + \frac{\partial \phi_y^i}{\partial x})$$

$$M^i_{xx} = B^i_{11}(\frac{\partial u_0^i}{\partial x}) + F^i_{11}(\frac{\partial^2 w_0^i}{\partial x^2}) + G^i_{11}\frac{\partial \phi_x^i}{\partial x} + B^i_{12}\frac{\partial v_0^i}{\partial y} + F^i_{12}\frac{\partial^2 w_0^i}{\partial y^2} + G^i_{12}\frac{\partial \phi_y^i}{\partial y} + B^i_{16}(\frac{\partial u_0^i}{\partial y} + \frac{\partial v_0^i}{\partial x})$$
$$+F^i_{16}(2\frac{\partial^2 W_0^i}{\partial x\,\partial y}) + G^i_{16}(\frac{\partial \phi_x^i}{\partial y} + \frac{\partial \phi_y^i}{\partial x})$$

$$M^i_{yy} = B^i_{12}(\frac{\partial u_0^i}{\partial x}) + F^i_{12}\frac{\partial^2 w_0^i}{\partial x^2} + G^i_{12}\frac{\partial \phi_x^i}{\partial x} + B^i_{22}(\frac{\partial v_0^i}{\partial y}) + F^i_{22}(\frac{\partial^2 w_0^i}{\partial y^2}) + G^i_{22}(\frac{\partial \phi_y^i}{\partial y}) + B^i_{26}(\frac{\partial u_0^i}{\partial y} + \frac{\partial v_0^i}{\partial x})$$
$$+F^i_{26}(2\frac{\partial^2 W_0^i}{\partial x\,\partial y}) + G^i_{26}(\frac{\partial \phi_x^i}{\partial y} + \frac{\partial \phi_y^i}{\partial x})$$

$$M^i_{xy} = B^i_{16}(\frac{\partial u_0^i}{\partial x}) + F^i_{16}(\frac{\partial^2 w_0^i}{\partial x^2}) + G^i_{16}\frac{\partial \phi_x^i}{\partial x} + B^i_{26}\frac{\partial v_0^i}{\partial y} + F^i_{26}\frac{\partial^2 w_0^i}{\partial y^2} + G^i_{26}\frac{\partial \phi_y^i}{\partial y} + B^i_{66}(\frac{\partial u_0^i}{\partial y} + \frac{\partial v_0^i}{\partial x})$$
$$+F^i_{66}(2\frac{\partial^2 W_0^i}{\partial x\,\partial y}) + G^i_{66}(\frac{\partial \phi_x^i}{\partial y} + \frac{\partial \phi_y^i}{\partial x})$$

$$P^i_{xx} = E^i_{11}(\frac{\partial u_0^i}{\partial x}) + G^i_{11}(\frac{\partial^2 w_0^i}{\partial x^2}) + H^i_{11}\frac{\partial \phi_x^i}{\partial x} + E^i_{12}\frac{\partial v_0^i}{\partial y} + G^i_{12}\frac{\partial^2 w_0^i}{\partial y^2} + H^i_{12}\frac{\partial \phi_y^i}{\partial y} + E^i_{16}(\frac{\partial u_0^i}{\partial y} + \frac{\partial v_0^i}{\partial x})$$
$$+G^i_{16}(2\frac{\partial^2 W_0^i}{\partial x\,\partial y}) + H^i_{16}(\frac{\partial \phi_x^i}{\partial y} + \frac{\partial \phi_y^i}{\partial x})$$

$$P^i_{yy} = E^i_{12}(\frac{\partial u_0^i}{\partial x}) + G^i_{12}\frac{\partial^2 w_0^i}{\partial x^2} + H^i_{12}\frac{\partial \phi_x^i}{\partial x} + E^i_{22}(\frac{\partial v_0^i}{\partial y}) + G^i_{22}(\frac{\partial^2 w_0^i}{\partial y^2}) + H^i_{22}(\frac{\partial \phi_y^i}{\partial y}) + E^i_{26}(\frac{\partial u_0^i}{\partial y} + \frac{\partial v_0^i}{\partial x})$$
$$+G^i_{26}(2\frac{\partial^2 W_0^i}{\partial x\,\partial y}) + H^i_{26}(\frac{\partial \phi_x^i}{\partial y} + \frac{\partial \phi_y^i}{\partial x})$$

$$P^i_{xy} = E^i_{16}(\frac{\partial u_0^i}{\partial x}) + G^i_{16}(\frac{\partial^2 w_0^i}{\partial x^2}) + H^i_{16}\frac{\partial \phi_x^i}{\partial x} + E^i_{26}\frac{\partial v_0^i}{\partial y} + G^i_{26}\frac{\partial^2 w_0^i}{\partial y^2} + H^i_{26}\frac{\partial \phi_y^i}{\partial y} + E^i_{66}(\frac{\partial u_0^i}{\partial y} + \frac{\partial v_0^i}{\partial x})$$
$$+G^i_{66}(2\frac{\partial^2 W_0^i}{\partial x\,\partial y}) + H^i_{66}(\frac{\partial \phi_x^i}{\partial y} + \frac{\partial \phi_y^i}{\partial x})$$

$$N^i_{xz} = K_S[A^i_{45}(\frac{\partial w_0^i}{\partial y}) + B^i_{45}(\frac{\partial w_0^i}{\partial y}) + D^i_{45}\phi_y^i + A^i_{55}(\frac{\partial w_0^i}{\partial x}) + B^i_{55}(\frac{\partial w_0^i}{\partial x}) + D^i_{55}\phi_x^i]$$

$$R^i_{xz} = K_S[B^i_{45}(\frac{\partial w_0^i}{\partial y}) + F^i_{45}(\frac{\partial w_0^i}{\partial y}) + G^i_{45}\phi_y^i + B^i_{55}(\frac{\partial w_0^i}{\partial x}) + F^i_{55}(\frac{\partial w_0^i}{\partial x}) + G^i_{55}\phi_x^i]$$

$$S^i_{xz} = K_S[I^i_{45}(\frac{\partial w_0^i}{\partial y}) + G^i_{45}(\frac{\partial w_0^i}{\partial y}) + H^i_{45}\phi_y^i + I^i_{55}(\frac{\partial w_0^i}{\partial x}) + G^i_{55}(\frac{\partial w_0^i}{\partial x}) + H^i_{55}\phi_x^i]$$

$$N^i_{yz} = K_S[A^i_{44}(\frac{\partial w_0^i}{\partial y}) + B^i_{44}(\frac{\partial w_0^i}{\partial y}) + D^i_{44}\phi_y^i + A^i_{45}(\frac{\partial w_0^i}{\partial x}) + B^i_{45}(\frac{\partial w_0^i}{\partial x}) + D^i_{45}\phi_x^i]$$

$$R^i_{yz} = K_S[B^i_{44}(\frac{\partial w_0^i}{\partial y}) + F^i_{44}(\frac{\partial w_0^i}{\partial y}) + G^i_{44}\phi_y^i + B^i_{45}(\frac{\partial w_0^i}{\partial x}) + F^i_{45}(\frac{\partial w_0^i}{\partial x}) + G^i_{45}\phi_x^i]$$

$$S^i_{yz} = K_S[J^i_{44}(\frac{\partial w_0^i}{\partial y}) + G^i_{44}(\frac{\partial w_0^i}{\partial y}) + H^i_{44}\phi_y^i + A^i_{45}(\frac{\partial w_0^i}{\partial x}) + G^i_{45}(\frac{\partial w_0^i}{\partial x}) + H^i_{45}\phi_x^i]$$

In the above equations,some of the stiffness coefficients for multilayer sheets are defined as follows:

$$\begin{gathered}
\int_{-h_i/2}^{h_i/2} \overline{Q}_{11} dZ_i = A^i{}_{11}, \int_{-h_i/2}^{h_i/2} \overline{Q}_{11} f_1(z_i) dZ_i = B^i{}_{11}, \int_{-h_i/2}^{h_i/2} \overline{Q}_{(11)} f_2(z_i) dZ_i = D^i{}_{11} \\
\int_{-h_i/2}^{h_i/2} \overline{Q}_{22} dZ_i = A^i{}_{22}, \int_{-h_i/2}^{h_i/2} \overline{Q}_{22} f_1(z_i) dZ = B^i{}_{22}, \int_{-h_i/2}^{h_i/2} \overline{Q}_{22} f_2(z_i) dZ_i = D^i{}_{22} \\
\int_{-h_i/2}^{h_i/2} \overline{Q}_{11} f_1(z_i) dZ_i = B^i{}_{11}, \int_{-h_i/2}^{h_i/2} \overline{Q}_{11} f_1(z_i) f_1(z_i) dZ = F^i{}_{11}, \int_{-h_i/2}^{h_i/2} \overline{Q}_{11} f_2(z_i) f_1(z_i) dZ_i = G^i{}_{11} \\
\int_{-h_i/2}^{h_i/2} \overline{Q}_{66} f_1(z_i) dZ_i = B^i{}_{66}, \int_{-h_i/2}^{h_i/2} \overline{Q}_{66} f_1(z_i) f_1(z_i) dZ_i = F^i{}_{66}, \int_{-h_i/2}^{h_i/2} \overline{Q}_{66} f_2(z_i) f_1(z_i) dZ_i = G^i{}_{66}
\end{gathered} \tag{19}$$

$$\begin{gathered}
\int_{-h_i/2}^{h_i/2} \overline{Q}_{44} dZ_i = A^i{}_{44}, \int_{-h_i/2}^{h_i/2} \overline{Q}_{44} \frac{df_1(z_i)}{dz_i} dZ_i = B^i{}_{44}, \int_{-h_i/2}^{h_i/2} \overline{Q}_{44} \frac{df_2(z_i)}{dz_i} dZ_i = D^i{}_{44} \\
\int_{-h_i/2}^{h_i/2} \overline{Q}_{45} dZ_i = A^i{}_{45}, \int_{-h_i/2}^{h_i/2} \overline{Q}_{45} \frac{df_1(z_i)}{dz_i} dZ_i = B^i{}_{45}, \int_{-h_i/2}^{h_i/2} \overline{Q}_{45} \frac{df_2(z_i)}{dz_i} dZ_i = D^i{}_{45} \\
\int_{-h_i/2}^{h_i/2} \overline{Q}_{44} \frac{df_1(z_i)}{dz_i} dZ_i = B^i{}_{44}, \int_{-h_i/2}^{h_i/2} \overline{Q}_{44} \frac{df_1(z_i)}{dz_i} \frac{df_1(z_i)}{dz_i} dZ_i = F^i{}_{44}, \\
\int_{-h_i/2}^{h_i/2} \overline{Q}_{44} \frac{df_2(z_i)}{dz_i} \frac{df_1(z_i)}{dz_i} dZ_i = G^i{}_{44}, \int_{-h_i/2}^{h_i/2} \overline{Q}_{45} \frac{df_1(z_i)}{dz_i} dZ_i = B^i{}_{45}, \\
\int_{-h_i/2}^{h_i/2} \overline{Q}_{45} \frac{df_1(z_i)}{dz_i} \frac{df_1(z_i)}{dz_i} dZ_i = F^i{}_{45}, \int_{-h_i/2}^{h_i/2} \overline{Q}_{45} \frac{df_2(z_i)}{dz_i} \frac{df_1(z_i)}{dz_i} dZ_i = G^i{}_{45}
\end{gathered} \tag{20}$$

The moment of inertia of the core is as follows:

$$I_n^c = \int_{-h_c/2}^{h_c/2} \rho_c z_c^n dz_c \quad , \quad n = 0,1,....6 \tag{21}$$

Also the moment of inertia of the face sheets in relation is:

$$\begin{gathered}
I_0^t = \int_{-h_t/2}^{h_t/2} \rho_t dz_t, \; I_1^t = \int_{-h_t/2}^{h_t/2} \rho_t f_1(z_i) dz_t, \; I_2^t = \int_{-h_t/2}^{h_t/2} \rho_t f_2(z_i) dz_t, \; I_3^t = \int_{-h_t/2}^{h_t/2} \rho_t f_1(z_i) f_2(z_i) dz_t \\
I_4^t = \int_{-h_t/2}^{h_t/2} \rho_t [f_2(z_i)]^2 dz_t, \; I_0^b = \int_{-h_b/2}^{h_b/2} \rho_b dz_b, \; I_1^b = \int_{-h_b/2}^{h_b/2} \rho_b f_1(z_i) dz_b, \; I_2^b = \int_{-h_b/2}^{h_b/2} \rho_b f_2(z_i) dz_b, \\
I_3^b = \int_{-h_b/2}^{h_b/2} \rho_b f_1(z_i) f_2(z_i) dz_b, \; I_4^b = \int_{-h_b/2}^{h_b/2} \rho_b [f_2(z_i)]^2 dz_b
\end{gathered} \tag{22}$$

2.5 Applying the Hamiltonian principle

To obtain the equations governing motion we use the Hamiltonian [34] principle which states:

$$\int_0^t \delta L dt = \int_0^t \left(\delta K - \delta U + \delta W_{ext}\right) dt = 0 \tag{23}$$

where, δK represents the kinetic energy changes, δU denotes the potential energy changes, and δW_{ext} shows the energy changes caused by the forces on the problem. δW_{ext} is zero due to the analysis of free vibrations.

$$\delta W_{ext} = 0 \tag{24}$$

The kinetic energy variations, assuming homogeneous conditions for displacement and velocity with respect to the time coordinate for a sandwich plate, can be generalized as:

$$\begin{aligned}
&\delta K = -\sum_{i=t,b,c}\left[\iint_{A_i}\int_{-\frac{h_i}{2}}^{\frac{h_i}{2}} \rho_i\left(\ddot{u}_i\delta u_i + \ddot{v}_i\delta v_i + \ddot{w}_i\delta w_i\right)dz_i dA_i\right]\\
&dA_c = dx_c dy_c, \qquad dA_i = dx_i dy_i, \qquad (i=t,b)
\end{aligned} \tag{25}$$

The first variation of internal potential energy of the sandwich panel is as follows [39]:

$$\begin{aligned}
&\delta U = \sum_{i=t,b}\left(\int_{v_i}\left(\sigma^i_{xx}\delta\varepsilon^i_{xx} + \sigma^i_{yy}\delta\varepsilon^i_{yy} + \tau^i_{xz}\delta\gamma^i_{xz} + \tau^i_{xy}\delta\gamma^i_{xy} + \tau^i_{yz}\delta\gamma^i_{yz}\right)dV_i\right) +\\
&\int_{v_c}\left(\sigma^c_{xx}\delta\varepsilon^c_{xx} + \sigma^c_{yy}\delta\varepsilon^c_{yy} + \sigma^c_{zz}\delta\varepsilon^c_{zz} + \tau^c_{xy}\delta\gamma^c_{xy} + \tau^c_{xz}\delta\gamma^c_{xz} + \tau^c_{yz}\delta\gamma^c_{yz}\right)dV_c\\
&dV_c = dA_c dZ_c = dx_c dy_c, dz_c, \qquad dV_i = dA_i dZ_i = dx_i dy_i, dz_i, \qquad (i=t,b)
\end{aligned} \tag{26}$$

Finally, the equations of motion for the flat sandwich plate with the ER core are obtained as a partial differential equation with 15 equations and 15 unknowns by replacing the stress relations, the resulting stresses and the moment of inertia of the core and the face sheet (Eqs. (18-8)), as well as the substitution of the relations of the displacement fields and the strain-displacement relations (terms (7-1)) in the relations of kinetic energy changes and system potentials (relationships (20-21)), along with using the Hamiltonian principle (relation (20)) and the fundamental principle of the calculus of variations.

$$\begin{aligned}
&\delta U^t_0:\\
&\frac{\partial N^t_{xx}}{\partial x} + \frac{\partial N^t_{xy}}{\partial y} + \frac{2}{h_c^2}\frac{\partial M^c_{2xx}}{\partial x} + \frac{4}{h_c^2}\frac{\partial M^c_{2xy}}{\partial y} + \frac{2}{h_c^2}\frac{\partial M^c_{2xy}}{\partial y} - \frac{4M^c_{1xz}}{h_c^2} - \frac{12M^c_{2xz}}{h_c^2} + \frac{4}{h_c^2}\frac{\partial M^c_{2xx}}{\partial x} =\\
&\left(-\frac{16I^c_5}{h_c^5} - \frac{8I^c_4}{h_c^4} + \frac{4I^c_3}{h_c^3} + \frac{2I^c_2}{h_c^2}\right)\ddot{u}^c_0 + \left(\frac{2I^c_3}{h_c^2} - \frac{8I^c_5}{h_c^4} - \frac{16I^c_6}{h_c^5} + \frac{4I^c_4}{h_c^3}\right)\ddot{u}^c_1 + \left(\frac{4I^c_4}{h_c^4} - \frac{16I^c_6}{h_c^6}\right)\ddot{u}^b_b +\\
&\left(\frac{16I^c_6}{h_c^6} + \frac{4I^c_4}{h_c^4} + \frac{16I^c_5}{h_c^5} + I^t_0\right)\ddot{u}^t_0 + \left(\frac{2I^c_4 h_b}{h_c^4} - \frac{8h_b I^c_6}{h_c^6}\right)\ddot{\phi}^b_x + \left(-\frac{8h_t I^c_5}{h_c^5} + I^t_2 - \frac{2I^c_4 h_t}{h_c^4} - \frac{8h_t I^c_6}{h_c^6}\right)\ddot{\phi}^t_x + I^t_1\ddot{w}^t_{0,x}
\end{aligned} \tag{27}$$

$$\begin{aligned}
&\delta U^b_0:\\
&\frac{\partial N^b_{xx}}{\partial x} + \frac{\partial N^b_{xy}}{\partial y} + \frac{2}{h_c^2}\frac{\partial M^c_{2xy}}{\partial y} - \frac{4}{h_c^3}\frac{\partial M^c_{3xx}}{\partial x} + \frac{2}{h_c^2}\frac{\partial M^c_{2xx}}{\partial x} - \frac{4M^c_{3xz}}{h_c^3} + \frac{12M^c_{2xz}}{h_c^3} =\\
&\left(\frac{16I^c_5}{h_c^5} + \frac{2I^c_2}{h_c^2} - \frac{8I^c_4}{h_c^4} - \frac{4I^c_3}{h_c^3}\right)\ddot{u}^c_0 + \left(-\frac{4I^c_4}{h_c^3} + \frac{2I^c_3}{h_c^2} - \frac{8I^c_5}{h_c^4} + \frac{16I^c_6}{h_c^5}\right)\ddot{u}^c_1 + \left(-\frac{16I^c_6}{h_c^6} + \frac{4I^c_4}{h_c^4}\right)\ddot{u}^t_0 +\\
&\left(I^b_0 + \frac{4I^c_4}{h_c^4} + \frac{16I^c_6}{h_c^6} - \frac{16I^c_5}{h_c^5}\right)\ddot{u}^b_0 + \left(I^b_2 - \frac{8h_b I^c_5}{h_c^5} + \frac{2I^c_4 h_b}{h_c^4} + \frac{8h_b I^c_6}{h_c^6}\right)\ddot{\phi}^b_x + \left(-\frac{2h_t I^c_4}{h_c^4} + \frac{8h_t I^c_6}{h_c^6}\right)\ddot{\phi}^t_x + I^b_1\ddot{w}^t_{0,x}
\end{aligned} \tag{28}$$

$$\begin{aligned}
&\delta V^t_0:\\
&\frac{\partial N^t_{yy}}{\partial y} + \frac{\partial N^t_{xy}}{\partial x} + \frac{2}{h_c^2}\frac{\partial M^c_{2yy}}{\partial y} + \frac{4}{h_c^3}\frac{\partial M^c_{3yy}}{\partial y} + \frac{2}{h_c^2}\frac{\partial M^c_{2xy}}{\partial x} + \frac{4}{h_c^3}\frac{\partial M^c_{3xy}}{\partial x} - \frac{4M^c_{1yz}}{h_c^2} - \frac{12M^c_{2yz}}{h_c^3} =\\
&\left(-\frac{16I^c_5}{h_c^5} - \frac{8I^c_4}{h_c^4} + \frac{4I^c_3}{h_c^3} + \frac{2I^c_2}{h_c^2}\right)\ddot{v}^c_0 + \left(\frac{2I^c_3}{h_c^3} - \frac{8I^c_5}{h_c^4} - \frac{16I^c_6}{h_c^5} + \frac{4I^c_4}{h_c^3}\right)\ddot{v}^c_1 + \left(\frac{4I^c_4}{h_c^4} - \frac{16I^c_6}{h_c^6}\right)\ddot{v}^b_0 +\\
&\left(I^t_0 + \frac{16I^c_6}{h_c^6} + \frac{4I^c_4}{h_c^4} + \frac{16I^c_5}{h_c^5}\right)\ddot{v}^t_0 + \left(\frac{2h_b I^c_4}{h_c^4} - \frac{8h_b I^c_6}{h_c^6}\right)\ddot{\phi}^b_y + \left(I^t_2 - \frac{8h_t I^c_5}{h_c^5} - \frac{2I^c_4 h_t}{h_c^4} - \frac{8h_t I^c_6}{h_c^6}\right)\ddot{\phi}^t_y + I^t_1\ddot{w}^t_{0,y}
\end{aligned} \tag{29}$$

$\delta V_0^{\,b}:$

$$\frac{\partial N_{yy}^{b}}{\partial y}+\frac{\partial N_{xy}^{b}}{\partial x}+\frac{2}{h_c^2}\frac{\partial M_{2yy}^{c}}{\partial y}-\frac{4}{h_c^3}\frac{\partial M_{3yy}^{c}}{\partial y}+\frac{2}{h_c^2}\frac{\partial M_{2xy}^{c}}{\partial x}-\frac{4}{h_c^3}\frac{\partial M_{3xy}^{c}}{\partial x}-\frac{4M_{1yz}^{c}}{h_c^2}+\frac{12M_{2yz}^{c}}{h_c^3}=$$
$$\left(\frac{16I_5^c}{h_c^5}+\frac{2I_2^c}{h_c^2}-\frac{8I_4^c}{h_c^4}-\frac{4I_4^c}{h_c^3R_{yc}}-\frac{4I_3^c}{h_c^3}\right)\ddot{v}_0^c+\left(-\frac{4I_4^c}{h_c^3}+\frac{2I_3^c}{h_c^2}-\frac{8I_5^c}{h_c^4}+\frac{16I_6^c}{h_c^5}\right)\ddot{v}_1^c+\left(I_0^b+\frac{4I_4^c}{h_c^4}+\frac{16I_6^c}{h_c^6}-\frac{16I_5^c}{h_c^5}\right)\ddot{v}_0^b+$$
$$\left(-\frac{16I_6^c}{h_c^6}+\frac{4I_4^c}{h_c^4}\right)\ddot{v}_0^t+\left(-\frac{8h_bI_5^c}{h_c^5}+\frac{2I_4^ch_b}{h_c^4}+\frac{8h_bI_6^c}{h_c^6}+I_2^b\right)\ddot{\phi}_y^b+\left(-\frac{2h_tI_4^c}{h_c^4}+\frac{8h_tI_6^c}{h_c^6}\right)\ddot{\phi}_y^t+I_1^b\ddot{w}_{0,x}^{\,b} \tag{30}$$

$\delta W_0^{\,t}:$

$$\frac{\partial N_{yz}^{t}}{\partial y}+\frac{\partial N_{xz}^{t}}{\partial x}-\frac{R_z^c}{h_c}-\frac{4M_z^c}{h_c^2}+\frac{2}{h_c^2}\frac{\partial M_{2xz}^{c}}{\partial y}+\frac{1}{h_c}\frac{\partial M_{1xz}^{c}}{\partial x}+\frac{1}{h_c}\frac{\partial M_{1yz}^{c}}{\partial y}+\frac{\partial^2 M_{xx}^{t}}{\partial x^2}+\frac{\partial^2 M_{yy}^{t}}{\partial y^2}-\frac{2\partial^2 M_{xy}^{t}}{\partial x^2}+\frac{\partial R_{xz}^{t}}{\partial x}+\frac{\partial R_{yz}^{t}}{\partial y}=$$
$$\left(-\frac{8I_4^c}{h_c^4}+\frac{I_1^c}{h_c}+\frac{2I_2^c}{h_c^2}-\frac{4I_3^c}{h_c^3}\right)\ddot{w}_0^{\,c}+\left(I_0^t+\frac{4I_4^c}{h_c^4}+\frac{I_2^c}{h_c^2}+\frac{4I_3^c}{h_c^3}\right)\ddot{w}_0^{\,t}+\left(\frac{4I_4^c}{h_c^4}-\frac{I_2^c}{h_c^2}\right)\ddot{w}_0^{\,b} \tag{31}$$

$\delta W_0^{\,b}:$

$$-\frac{1}{h_c}\frac{\partial M_{1xz}^{c}}{\partial x}-\frac{1}{h_c}\frac{\partial M_{1yz}^{c}}{\partial y}+\frac{\partial N_{xz}^{b}}{\partial x}+\frac{\partial N_{yz}^{b}}{\partial y}+\frac{R_z^c}{h_c}-\frac{4M_z^c}{h_c^2}+\frac{2}{h_c^2}\frac{\partial M_{2xz}^{c}}{\partial x}+\frac{2}{h_c^2}\frac{\partial M_{2yz}^{c}}{\partial y}+\frac{\partial^2 M_{xx}^{b}}{\partial x^2}+\frac{\partial^2 M_{yy}^{b}}{\partial y^2}-\frac{2\partial^2 M_{xy}^{b}}{\partial x^2}+\frac{\partial R_{xz}^{0}}{\partial x}+\frac{\partial R_{yz}^{b}}{\partial y}=$$
$$\left(\frac{4I_3^c}{h_c^3}-\frac{8I_4^c}{h_c^4}-\frac{I_1^c}{h_c}+\frac{2I_2^c}{h_c^2}\right)\ddot{w}_0^{\,c}+\left(I_0^b+\frac{4I_4^c}{h_c^4}+\frac{I_2^c}{h_c^2}-\frac{4I_3^c}{h_c^3}\right)\ddot{w}_0^{\,b}+\left(\frac{4I_4^c}{h_c^4}-\frac{I_2^c}{h_c^2}\right)\ddot{w}_0^{\,t} \tag{32}$$

$\delta\phi_x^t:$

$$\frac{\partial P_{xx}^t}{\partial x}-\frac{h_t}{h_c^2}\frac{\partial M_{2xy}^{c}}{\partial y}+\frac{\partial P_{xy}^t}{\partial y}-S_{xz}^{\,t}-\frac{h_t}{h_c^2}\frac{\partial M_{2xx}^{c}}{\partial x}-\frac{2h_t}{h_c^3}\frac{\partial M_{3xx}^{c}}{\partial x}-\frac{2h_t}{h_c^3}\frac{\partial M_{3xy}^{c}}{\partial y}+\frac{2h_tM_{1xz}^{c}}{h_c^2}+\frac{6h_tM_{2xz}^{c}}{h_c^3}=$$
$$\left(-\frac{h_tI_2^c}{h_c^2}-\frac{2h_tI_3^c}{h_c^3}+\frac{8h_tI_5^c}{h_c^5}+\frac{4h_tI_4^c}{h_c^4}\right)\ddot{u}_0^c+\left(-\frac{h_tI_3^c}{h_c^2}-\frac{2h_tI_4^c}{h_c^3}+\frac{4I_5^ch_t}{h_c^4}+\frac{8I_6^ch_t}{h_c^5}\right)\ddot{u}_1^c+\left(-\frac{2h_tI_4^c}{h_c^4}+\frac{8I_6^ch_t}{h_c^6}\right)\ddot{u}_0^b+$$
$$\left(-\frac{2I_4^ch_t}{h_c^4}+\frac{8I_5^ch_t}{h_c^5}-\frac{8I_6^ch_t}{h_c^6}+I_2^t\right)\ddot{u}_0^t+I_3^t\ddot{w}_{0,x}^{\,t}+\left(-\frac{h_tI_4^ch_b}{h_c^4}+\frac{4h_bI_6^ch_t}{h_c^6}\right)\ddot{\phi}_x^b+\left(I_4^t+\frac{h_t^2I_4^c}{h_c^4}+\frac{4h_t^2I_5^c}{h_c^5}+\frac{4h_t^2I_6^c}{h_c^6}\right)\ddot{\phi}_x^t \tag{33}$$

$\delta\phi_x^b:$

$$\frac{h_b}{h_c^2}\frac{\partial M_{2xx}^{c}}{\partial x}+\frac{h_c}{h_c^2}\frac{\partial M_{2xy}^{c}}{\partial y}+\frac{\partial P_{xx}^c}{\partial x}+\frac{\partial P_{xy}^b}{\partial y}-S_{xz}^{\,b}-\frac{2h_b}{h_c^3}\frac{\partial M_{3xx}^{c}}{\partial x}-\frac{2h_b}{h_c^3}\frac{\partial M_{3xy}^{c}}{\partial y}-\frac{2h_bM_{1xz}^{c}}{h_c^2}+\frac{2h_tM_{1xz}^{c}}{h_c^2}+\frac{6h_bM_{2xz}^{c}}{h_c^3}=$$
$$\left(\frac{I_2^ch_b}{h_c^2}-\frac{2h_bI_3^c}{h_c^3}+\frac{8h_bI_5^c}{h_c^5}-\frac{4h_bI_4^c}{h_c^4}\right)\ddot{u}_0^c+\left(\frac{h_bI_3^c}{h_c^2}-\frac{2h_bI_4^c}{h_c^3}-\frac{4I_5^ch_b}{h_c^4}+\frac{8I_6^ch_b}{h_c^5}\right)\ddot{u}_1^c+\left(-\frac{8I_5^ch_b}{h_c^5}+\frac{2h_bI_4^c}{h_c^4}+\frac{8I_6^ch_b}{h_c^6}+I_2^b\right)\ddot{u}_0^b$$
$$+I_3^b\ddot{w}_{0,x}^{\,b}+\left(\frac{2h_bI_4^c}{h_c^4}-\frac{8I_6^ch_b}{h_c^6}\right)\ddot{u}_0^t+\left(\frac{h_b^2I_4^c}{h_c^4}-\frac{4h_b^2I_5^c}{h_c^5}+I_4^b+\frac{4h_b^2I_6^c}{h_c^6}\right)\ddot{\phi}_x^b+\left(-\frac{h_bI_4^ch_t}{h_c^4}+\frac{4h_th_bI_6^c}{h_c^6}\right)\ddot{\phi}_x^t \tag{34}$$

$\delta\phi_y^t:$

$$-\frac{h_t}{h_c^2}\frac{\partial M_{2yy}^{c}}{\partial y}+\frac{\partial P_{yy}^t}{\partial y}+\frac{\partial P_{xy}^t}{\partial x}-S_{yz}^{\,t}-\frac{2h_t}{h_c^3}\frac{\partial M_{3yy}^{c}}{\partial y}-\frac{h_t}{h_c^2}\frac{\partial M_{2xy}^{c}}{\partial x}-\frac{2h_t}{h_c^3}\frac{\partial M_{3xy}^{c}}{\partial x}+\frac{2h_tM_{1yz}^{c}}{h_c^2}+\frac{6h_tM_{2yz}^{c}}{h_c^3}=$$
$$\left(-\frac{h_tI_2^c}{h_c^2}-\frac{2h_tI_3^c}{h_c^3}+\frac{8h_tI_5^c}{h_c^5}+\frac{4h_tI_4^c}{h_c^4}\right)\ddot{v}_0^c+\left(-\frac{h_tI_3^c}{h_c^2}-\frac{2h_tI_4^c}{h_c^3}+\frac{4I_5^ch_t}{h_c^4}+\frac{8I_6^ch_t}{h_c^5}\right)\ddot{v}_1^c+\left(-\frac{2h_tI_4^c}{h_c^4}+\frac{8I_6^ch_t}{h_c^6}\right)\ddot{v}_0^b$$
$$+I_3^t\ddot{w}_{0,y}^{\,b}+\left(-\frac{2I_4^ch_t}{h_c^4}+\frac{8I_5^ch_t}{h_c^5}-\frac{8I_6^ch_t}{h_c^6}+I_2^t\right)\ddot{v}_0^t+\left(-\frac{h_th_bI_4^c}{h_c^4}+\frac{4h_bh_tI_6^c}{h_c^6}\right)\ddot{\phi}_y^b+\left(I_4^t+\frac{h_t^2I_4^c}{h_c^4}+\frac{4h_t^2I_5^c}{h_c^5}+\frac{4h_t^2I_6^c}{h_c^6}\right)\ddot{\phi}_y^t \tag{35}$$

$$
\begin{aligned}
&\delta\phi_y^b :\\
&\frac{h_b}{h_c^2}\frac{\partial M_{2yy}^c}{\partial y}+\frac{\partial M_{yy}^b}{\partial y}+\frac{\partial M_{xy}^b}{\partial x}-N_{yz}^b-\frac{2h_b}{h_c^3}\frac{\partial M_{3yy}^c}{\partial y}+\frac{h_b}{h_c^2}\frac{\partial M_{2xy}^c}{\partial x}-\frac{2h_b}{h_c^3}\frac{\partial M_{3xy}^c}{\partial x}-\frac{2h_b M_{1yz}^c}{h_c^2}+\frac{6h_b M_{2yz}^c}{h_c^3}=\\
&\left(\frac{h_b I_2^c}{h_c^2}-\frac{2h_b I_3^c}{h_c^3}+\frac{8h_b I_5^c}{h_c^5}-\frac{4h_b I_4^c}{h_c^4}\right)\ddot{v}_0^c+\left(\frac{h_b I_3^c}{h_c^2}-\frac{2h_b I_4^c}{h_c^3}-\frac{4I_5^c h_b}{h_c^4}+\frac{8I_6^c h_b}{h_c^5}\right)\ddot{v}_1^c+\left(\frac{2h_b I_4^c}{h_c^4}-\frac{8I_6^c h_b}{h_c^6}\right)\ddot{v}_0^t\\
&+\left(I_2^b-\frac{8I_5^c h_b}{h_c^5}+\frac{2I_4^c h_b}{h_c^4}+\frac{8I_6^c h_b}{h_c^6}\right)\ddot{v}_0^b+\left(I_4^b+\frac{h_b I_4^c}{h_c^4}-\frac{4h_b^2 I_5^c}{h_c^5}+\frac{4h_b^2 I_6^c}{h_c^6}\right)\ddot{\phi}_y^b+\left(-\frac{h_b h_t I_4^c}{h_c^4}+\frac{4h_b h_t I_6^c}{h_c^6}\right)\ddot{\phi}_y^t
\end{aligned}
\tag{36}
$$

$$
\begin{aligned}
&\delta U_0^c :\\
&\frac{\partial N_{xx}^c}{\partial x}+\frac{\partial N_{xy}^c}{\partial y}-\frac{4}{h_c^2}\frac{\partial M_{2xy}^c}{\partial y}-\frac{4}{h_c^2}\frac{\partial M_{2xx}^c}{\partial x}+\frac{8M_{1xz}^c}{h_c^2}=\left(I_0^c-\frac{8I_2^c}{h_c^2}+\frac{16I_4^c}{h_c^4}\right)\ddot{u}_0^c+\left(I_1^c-\frac{8I_3^c}{h_c^2}+\frac{16I_5^c}{h_c^4}\right)\ddot{u}_1^c+\left(\frac{2I_2^c}{h_c^2}-\frac{8I_4^c}{h_c^4}+\frac{16I_5^c}{h_c^5}-\frac{4I_3^c}{h_c^3}\right)\ddot{u}_0^b\\
&+\left(\frac{4I_3^c}{h_c^3}-\frac{16I_5^c}{h_c^5}+\frac{2I_2^c}{h_c^2}-\frac{8I_4^c}{h_c^4}\right)\ddot{u}_0^t+\left(\frac{h_b I_2^c}{h_c^2}-\frac{4h_b I_4^c}{h_c^4}-\frac{2h_b I_3^c}{h_c^3}+\frac{8h_b I_5^c}{h_c^5}\right)\ddot{\phi}_x^b+\left(-\frac{h_t I_2^c}{h_c^2}+\frac{4h_t I_4^c}{h_c^4}-\frac{2h_t I_3^c}{h_c^3}+\frac{8h_t I_5^c}{h_c^5}\right)\ddot{\phi}_x^t
\end{aligned}
\tag{37}
$$

$$
\begin{aligned}
&\delta U_1^c :\\
&\frac{\partial M_{1xx}^c}{\partial x}-\frac{4}{h_c^2}\frac{\partial M_{3xx}^c}{\partial x}+\frac{\partial M_{1xy}^c}{\partial y}-\frac{4}{h_c^2}\frac{\partial M_{3xy}^c}{\partial y}-N_{xz}^c+\frac{12M_{2xz}^c}{h_c^2}=\left(I_1^c-\frac{16I_5^c}{h_c^4}-\frac{8I_3^c}{h_c^2}\right)\ddot{u}_0^c+\left(\frac{2I_3^c}{h_c^2}-\frac{4I_4^c}{h_c^3}+\frac{16I_6^c}{h_c^5}-\frac{8I_5^c}{h_c^4}\right)\ddot{u}_0^b+\\
&\left(I_2^c-\frac{8I_4^c}{h_c^2}+\frac{16I_6^c}{h_c^4}\right)\ddot{u}_1^c+\left(\frac{4I_4^c}{h_c^3}-\frac{16I_6^c}{h_c^5}+\frac{2I_3^c}{h_c^2}-\frac{8I_5^c}{h_c^4}\right)\ddot{u}_0^t+\left(\frac{I_3^c h_b}{h_c^2}-\frac{4h_b I_5^c}{h_c^4}-\frac{2h_b I_4^c}{h_c^3}+\frac{8h_b I_6^c}{h_c^5}\right)\ddot{\phi}_x^b+\\
&\left(\frac{I_3^c h_t}{h_c^2}+\frac{4h_t I_5^c}{h_c^4}-\frac{2h_t I_4^c}{h_c^3}+\frac{8h_t I_6^c}{h_c^5}\right)\ddot{\phi}_x^t+\left(-\frac{h_t I_2^c}{h_c^2}+\frac{4h_t I_4^c}{h_c^4}-\frac{2h_t I_3^c}{h_c^3}+\frac{8h_t I_5^c}{h_c^5}\right)\ddot{\phi}_x^t
\end{aligned}
\tag{38}
$$

$$
\begin{aligned}
&\delta V_0^c :\\
&\frac{\partial N_{yy}^c}{\partial y}+\frac{\partial N_{xy}^c}{\partial x}-\frac{4}{h_c^2}\frac{\partial M_{2xy}^c}{\partial x}-\frac{4}{h_c^2}\frac{\partial M_{2yy}^c}{\partial y}+\frac{8M_{1yz}^c}{h_c^2}=\left(\frac{16I_4^c}{h_c^4}+I_0^c-\frac{8I_2^c}{h_c^2}\right)\ddot{v}_0^c+\left(I_1^c-\frac{8I_3^c}{h_c^2}+\frac{16I_5^c}{h_c^4}\right)\ddot{v}_1^c+\\
&\left(\frac{2I_2^c}{h_c^2}-\frac{8I_4^c}{h_c^4}-\frac{4I_3^c}{h_c^3}+\frac{16I_5^c}{h_c^5}\right)\ddot{v}_0^b+\left(\frac{4I_3^c}{h_c^3}-\frac{16I_5^c}{h_c^5}+\frac{2I_2^c}{h_c^2}-\frac{8I_4^c}{h_c^4}\right)\ddot{v}_0^t+\left(\frac{h_b I_2^c}{h_c^2}-\frac{4h_b I_4^c}{h_c^4}-\frac{2h_b I_3^c}{h_c^3}+\frac{8h_b I_5^c}{h_c^5}\right)\ddot{\phi}_y^b+\\
&\left(-\frac{h_t I_2^c}{h_c^2}+\frac{4h_t I_4^c}{h_c^4}-\frac{2h_t I_3^c}{h_c^3}+\frac{8h_t I_5^c}{h_c^5}\right)\ddot{\phi}_y^t
\end{aligned}
\tag{39}
$$

$$
\begin{aligned}
&\delta V_1^c :\\
&\frac{\partial M_{1yy}^c}{\partial y}-\frac{4}{h_c^2}\frac{\partial M_{3yy}^c}{\partial y}+\frac{\partial M_{1xy}^c}{\partial x}-\frac{4}{h_c^2}\frac{\partial M_{3xy}^c}{\partial x}-N_{yz}^c+\frac{12M_{2yz}^c}{h_c^2}=\left(I_1^c+\frac{16I_5^c}{h_c^4}-\frac{8I_3^c}{h_c^2}\right)\ddot{v}_0^c+\left(\frac{2I_3^c}{h_c^2}-\frac{4I_4^c}{h_c^3}+\frac{16I_5^c}{h_c^5}-\frac{8I_5^c}{h_c^4}\right)\ddot{v}_0^b+\\
&\left(I_2^c-\frac{8I_4^c}{h_c^2}+\frac{16I_6^c}{h_c^4}\right)\ddot{v}_1^c+\left(\frac{4I_4^c}{h_c^3}-\frac{16I_6^c}{h_c^5}+\frac{2I_3^c}{h_c^2}-\frac{8I_5^c}{h_c^4}\right)\ddot{v}_0^t+\left(\frac{I_3^c h_b}{h_c^2}-\frac{4h_b I_5^c}{h_c^4}-\frac{2h_b I_4^c}{h_c^3}+\frac{8h_b I_6^c}{h_c^5}\right)\ddot{\phi}_y^b+\\
&\left(-\frac{I_2^c h_t}{h_c^2}+\frac{4h_t I_5^c}{h_c^4}-\frac{2h_t I_4^c}{h_c^3}+\frac{8h_t I_6^c}{h_c^5}\right)\ddot{\phi}_y^t
\end{aligned}
\tag{40}
$$

$$
\begin{aligned}
&\delta W_0^c :\\
&\frac{\partial N_{xz}^c}{\partial x}-\frac{4}{h_c^2}\frac{\partial M_{2xz}^c}{\partial x}-\frac{4}{h_c^2}\frac{\partial M_{2yz}^c}{\partial y}+\frac{\partial N_{yz}^c}{\partial y}+\frac{8}{h_c^2}M_z^c=\left(\frac{16I_4^c}{h_c^4}-\frac{8I_2^c}{h_c^2}+I_0^c\right)\ddot{w}_0^c+\left(\frac{2I_2^c}{h_c^2}-\frac{8I_4^c}{h_c^4}+\frac{I_1^c}{h_c}-\frac{4I_3^c}{h_c^3}\right)\ddot{w}_0^t+\\
&\left(\frac{2I_2^c}{h_c^2}-\frac{8I_4^c}{h_c^4}-\frac{I_1^c}{h_c}+\frac{4I_3^c}{h_c^3}\right)\ddot{w}_0^b
\end{aligned}
\tag{41}
$$

In order to express the equations of motion in terms of displacement terms and to facilitate the process of solving the equations of motion, the following integrals are defined.

$$
\begin{aligned}
&e_n^{c(xx)} = \int_{-h_c/2}^{h_c/2} Z_c E_{xx}^c(Z)dz && n = 0,1,2,3 \\
&e_n^{c(yy)} = \int_{-h_c/2}^{h_c/2} Z_c E_{yy}^c(Z)dz && n = 0,1,2,3 \\
&g_n^{c(xy)} = \int_{-h_c/2}^{h_c/2} Z_c^n G_{xy}^c(Z)dz && n = 0,1,2,3 \\
&g_n^{c(xz)} = \int_{-h_c/2}^{h_c/2} Z_c^n G_{xz}^c(Z)dz && n = 0,1,2 \\
&g_n^{c(yz)} = \int_{-h_c/2}^{h_c/2} Z_c^n G_{yz}^c(Z)dz && n = 0,1,2
\end{aligned}
\tag{42}
$$

By substituting relation (43) in relations (12), Constitutive equations for thick core layer can be written as:

$$
N_{xy}^c = g_0^{c(xy)}\frac{\partial v_0^c}{\partial x} + g_1^{c(xy)}\frac{\partial v_1^c}{\partial x} + g_2^{c(xy)}\frac{\partial v_2^c}{\partial x} + g_3^{c(xy)}\frac{\partial v_3^c}{\partial x} + g_0^{c(xy)}\frac{\partial u_0^c}{\partial y} + g_1^{c(xy)}\frac{\partial u_1^c}{\partial y} + g_2^{c(xy)}\frac{\partial u_2^c}{\partial y} + g_3^{c(xy)}\frac{\partial u_3^c}{\partial y} \tag{43}
$$

$$
\begin{aligned}
N_{xz}^c &= g_0^{c(xz)}u_1^c + 2g_1^{c(xz)}u_2^c + 3g_2^{c(xz)}u_3^c + g_0^{c(xz)}\frac{\partial W_0^c}{\partial x} + g_1^{c(xz)}\frac{\partial W_1^c}{\partial x} + g_2^{c(xz)}\frac{\partial W_2^c}{\partial x} \\
N_{yz}^c &= g_0^{c(yz)}v_1^c + 2g_1^{c(yz)}v_2^c + 3g_2^{c(yz)}v_3^c + g_0^{c(yz)}\frac{\partial W_0^c}{\partial y} + g_1^{c(yz)}\frac{\partial W_1^c}{\partial y} + g_2^{c(yz)}\frac{\partial W_2^c}{\partial y}
\end{aligned}
\tag{44}
$$

$$
\begin{aligned}
M_{nxx}^c &= e_n^{c(xx)}\frac{\partial u_0^c}{\partial x} + e_{n+1}^{c(xx)}\frac{\partial u_1^c}{\partial x} + e_{n+2}^{c(xx)}\frac{\partial u_2^c}{\partial x} + e_{n+3}^{c(xx)}\frac{\partial u_3^c}{\partial x} \\
M_{nyy}^c &= e_n^{c(yy)}\frac{\partial v_0^c}{\partial y} + e_{n+1}^{c(yy)}\frac{\partial v_1^c}{\partial y} + e_{n+2}^{c(yy)}\frac{\partial v_2^c}{\partial y} + e_{n+3}^{c(yy)}\frac{\partial v_3^c}{\partial y} \\
M_{nxy}^c &= g_n^{c(xy)}\frac{\partial v_0^c}{\partial x} + g_{n+1}^{c(xy)}\frac{\partial v_1^c}{\partial x} + g_{n+2}^{c(xy)}\frac{\partial v_2^c}{\partial x} + g_{n+3}^{c(xy)}\frac{\partial v_3^c}{\partial x} + g_n^{c(xy)}\frac{\partial u_0^c}{\partial y} + g_{n+1}^{c(xy)}\frac{\partial u_1^c}{\partial y} + g_{n+2}^{c(xy)}\frac{\partial u_2^c}{\partial y} + g_{n+3}^{c(xy)}\frac{\partial u_3^c}{\partial y}
\end{aligned}
\tag{45}
$$

$$
\begin{aligned}
M_{nxz}^c &= g_n^{c(xz)}u_1^c + 2g_{n+1}^{c(xz)}u_2^c + 3g_{n+2}^{c(xz)}u_3^c + g_n^{c(xz)}\frac{\partial W_0^c}{\partial x} + g_{n+1}^{c(xz)}\frac{\partial W_1^c}{\partial x} + g_{n+2}^{c(xz)}\frac{\partial W_2^c}{\partial x} \\
M_{nyz}^c &= g_n^{c(yz)}v_1^c + 2g_{n+1}^{c(yz)}v_2^c + 3g_{n+2}^{c(yz)}v_3^c + g_n^{c(yz)}\frac{\partial W_0^c}{\partial y} + g_{n+1}^{c(yz)}\frac{\partial W_1^c}{\partial y} + g_{n+2}^{c(yz)}\frac{\partial W_2^c}{\partial y}
\end{aligned}
\tag{46}
$$

$$
\begin{aligned}
R_z^c &= e_0^{c(xz)}w_1^c + 2e_1^{c(xz)}w_2^c \\
M_z^c &= e_1^{c(xz)}w_1^c + 2g_2^{c(xz)}w_2^c
\end{aligned}
\tag{47}
$$

According to the relationship (19) and (44-47) equations of plane motion are obtained based on displacements. In this study, simply supported boundary conditions are assumed for all four edges of the sandwich plate. It can be shown that the assumed responses of the relationship satisfy simply supported boundary conditions [17].

$$
\begin{bmatrix}
u_0^j(x,y,t) \\ v_0^j(x,y,t) \\ w_0^j(x,y,t) \\ \phi_x^j(x,y,t) \\ \phi_y^j(x,y,t) \\ u_k^c(x,y,t) \\ v_k^c(x,y,t) \\ w_0^c(x,y,t)
\end{bmatrix}
= \sum_{n=1}^{\infty}\sum_{m=1}^{\infty}
\begin{bmatrix}
U_{0mn}^j \cos(\alpha_m x)\sin(\beta_n y) \\
V_{0mn}^j \sin(\alpha_m x)\cos(\beta_n y) \\
W_{0mn}^j \sin(\alpha_m x)\sin(\beta_n y) \\
\phi_{xmn}^j \cos(\alpha_m x)\sin(\beta_n y) \\
\phi_{ymn}^j \sin(\alpha_m x)\cos(\beta_n y) \\
U_{kmn}^c \cos(\alpha_m x)\sin(\beta_n y) \\
V_{kmn}^c \sin(\alpha_m x)\cos(\beta_n y) \\
W_{lmn}^j \sin(\alpha_m x)\sin(\beta_n y)
\end{bmatrix}
e^{i\omega t} \qquad (k = 1,1,2,3),(l = 0,1,2) \tag{48}
$$

where $\alpha_m = \dfrac{m\pi}{a}$ and $\beta_n = \dfrac{n\pi}{b}$.

In Eq. (48), U^j_{0mn}, V^j_{0mn}, W^j_{0mn}, ϕ^j_{xmn}, ϕ^j_{ymn}, U^c_{kmn}, V^c_{kmn} and W^j_{lmn} are the Fourier coefficients while m and n represent half wave numbers along x and y directions, respectively. By replacing Eqs. (48) in the governing equations of motion, the governing equations are transformed into ordinary coupled differential equations:

$$[M]\{\ddot{c}\}+[K]\{c\}=\{0\},$$
$$\{c\}=\{u^t_{0mn}, u^b_{0mn}, v^t_{0mn}, v^b_{0mn}, w^t_{0mn}, w^b_{0mn}, \phi^t_{xmn}, \psi^b_{xmn}, \phi^t_{ymn}, \psi^b_{ymn}, u^c_{0mn}, u^c_{1mn}, v^c_{0mn}, v^c_{1mn}, w^c_{0mn}\} \tag{49}$$

Hence, the problem of free vibration of the sandwich plate with a simple support becomes the standard equation of structural response; [*K*] represents stiffness matrices and [*M*] shows matrices of mass. Finally, by assuming free vibrations, one can calculate the natural frequencies, ω, and modal damping coefficients η_v for different vibrational modes from Eqs. (45) [11-12]:

$$\omega=\sqrt{Re(\varpi^2)} \qquad \eta_v=\frac{Im(\varpi^2)}{Re(\varpi^2)} \tag{50}$$

3 RESULTS AND DISCUSSION

3.1 Validation of equations

Here are two examples for the structure and the results. To verify the equations obtained, we first compare the results obtained with the present work with the recent work in the literature and definitely with flexible core. Then, we review the results obtained with the ER core.

Example1: Flat sandwich panel with flexible core:

The mechanical and geometrical properties of the structure considered in this example are presented in Table 1. The upper and lower portions of the pure aluminum are [0,0,0] and the sheet is symmetrical to the middle plate.

Table 1
Mechanical and geometrical properties of flat sandwich sheets with flexible core [40].

Geometry	$a = 0.4\ m$	$b = 0.4\ m$	$h_c = 0.005\ m$	$h_t = h_b = 0.005\ m$
Core	$G = 4\ GPa$	$G_{13} = G_{23} = G\ (1+I\beta)$	$\beta = 0.38$	$\rho = 2000 kg/m^3$
Face sheets	$E_1 = E_2 = E_3 = 207GPa$	$G_{12} = G_{13} = G_{23} = 77.58GPa$	$v_{12} = v_{13} = v_{23} = 0.334$	$\rho = 7800 kg/m^3$

G: real part of the complex shear modulus
β :loss factor of the damping material

Table 2 provides the results of the present study for flat sandwich sheets with MR core using the improved high-order theory of sandwich sheets, and further compared with the results obtained from the classical high-order theory of multilayer sheets [8]. Exponential shear deformation theory is used in the face sheets of the present study.

Table 2
Normal frequency values first to fourth for flat sandwich sheets with flexible core. The lay-up sequences for face sheets were [0/core/0] and G = 4 *MPa* and $a/b = 1$, $h_c/h_t = 1$.

Natural frequency (*rad/s*)	Present model	modal factor	Reference [8]	modal factor	Reference [40]	modal factor	Error Difference(%)
(1,1)	974.716	0.04383	972.89	0.044	975.17	0.04431	0.047
(1,2)	2347.82	0.01910	2346.45	0.019	2350.79	0.01918	0.126
(2,1)	2347.82	0.01910	2346.45	0.019	2350.79	0.01918	0.126
(2,2)	3717.78	0.01221	3711.90	0.012	3725.33	0.1224	0.203

Example2: Flat sandwich plate with aluminum face sheet and ER smart liquid core:

The mechanical and geometrical properties of the structure in this example are presented in Table 3. The lay-up sequences for face sheets were [0/90/0] and the sandwich panel was symmetric about the mid-plane.

Table 3
Mechanical and geometrical properties of flat sandwich sheets with aluminum face sheet and ER core [2].

Geometry	$a = 0.4\ m$	$b = 0.4\ m$	$h_c = 0.5\ m$	$h_t = h_b = 0.5\ m$
Core	$G^{c}_{2b(xz)} = G'^{c}_{b(xz)} + G''^{c}_{b(xz)}$	$G^{c}_{2b(yz)} = G'^{c}_{b(yz)} + G''^{c}_{b(yz)}$	$G'^{c}_{\alpha(xz)} = G'^{c}_{b(yz)} = 50.000E^{2}$ $G''^{c}_{\alpha(xz)} = G''^{c}_{b(yz)} = 2600E + 1700$	$\rho = 1700 kg / m^{3}$
Face sheets	$E_1 = E_2 = E_3 = 70GPa$	$G_{12} = G_{13} = G_{23} = 26.9GPa$	$v_{12} = v_{13} = v_{23} = 0.3$	$\rho = 2700 kg / m^{3}$

Table 4 presents the results of the present study for flat sandwich sheets with ER core using the improved high-order theory of sandwich sheets, with the results obtained from the classical high-order theory of multilayer sheets [39]. Kirchhoff's theory has been used in the face sheet for reference [2].

Table 4
Normal frequency values first to fourth for flat sandwich sheets with Aluminum face sheet and ER Core. The lay-up sequences sheets were [0/core/0] for, $E = 0$, $a/b = 1$, $h_c / h_t = 1$.

Natural frequency (*rad/s*)	Present model	modal factor	Reference [2]	modal factor	Error Difference(%)
(1,1)	13.1929	0.01719	13.1925	0.0172	0.003
(1,2)	32.9808	0.0068	32.9808	0.0069	0.00
(2,1)	32.9808	0.0068	32.9808	0.0069	0.00
(2,2)	52.7686	0.0042	52.7693	0.0043	0.002

3.2 Free vibration analysis

In this section, the free vibrations of sandwich sheets with composite and ER core are investigated. The effects of changing the thickness of the ER layer and the electric field intensity are also examined on the natural frequencies of the sheet. The lay-up sequences for face sheets were [0/0/0/core/0/0/0] and the sandwich panel was symmetric about the mid-plane. Mechanical and geometrical properties of flat sandwich panel with aluminum face sheet and ER core is in Table 3. Table 5 presents the results of the present study for flat core sandwich sheets with ER core using the improved high-order theory of sandwich sheets, with the results obtained from the classical high-order theory of multilayer sheets [2]. Kirchhoff's theory has been used in the face sheets for reference [2].

Table 5
Normal frequency first-fourth frequency values and modal damping coefficients for the first four vibration modes for core thickness, field intensity, and different aspect ratio coefficients of flat sandwich sheets with aluminum face sheets and ER core plates.

			E=0.5 *KV/mm*		*E*=1.5 *KV/mm*		*E*=2 *KV/mm*		*E*=3.5 *KV/mm*	
Mode		*a/b*	$\omega^*(Hz)$	η_v	$\omega^*(Hz)$	η_v	$\omega^*(Hz)$	η_v	$\omega^*(Hz)$	η_v
(1,1)	1	1	13.9948	0.02641	18.8419	0.02317	21.8042	0.01871	29.7528	0.009341
		2	33.8013	0.01146	39.5583	0.01462	43.7319	0.01393	57.6382	0.0098
		4	112.96	0.0035	119.324	0.0057	124.53	0.0064	145.649	0.0067
	4	1	11.0131	0.0394	16.652	0.0308	20.2136	0.0248	31.1417	0.01398
		2	26.1349	0.0175	32.8503	0.0203	37.6871	0.0188	54.4442	0.0131
		4	86.5289	0.0054	94.0419	0.0085	100.127	0.0092	124.608	0.0091
(1,2)	1	1	33.8013	0.01146	39.5583	0.01462	43.7319	0.01393	57.6382	0.009828
		2	53.5933	0.0073	59.6525	0.01057	64.3118	0.01081	81.2693	0.0090
		4	132.746	0.0029	139.153	0.0049	144.445	0.0056	166.298	0.0062
	4	1	26.1349	0.0175	32.8503	0.02038	37.6871	0.0188	54.4442	0.01818
		2	41.2369	0.0112	48.3397	0.01516	53.7398	0.0149	73.6221	0.0119
		4	101.624	0.0046	109.197	0.0074	115.394	0.0082	140.74	0.0085
(2,1)	1	1	33.8013	0.01146	39.5583	0.01462	43.7319	0.01393	57.6382	0.009828
		2	112.96	0.0035	119.324	0.0057	124.53	0.00640	145.649	0.0067
		4	429.514	0.0009	436.101	0.001674	441.756	0.0020	467.177	0.0027
	4	1	26.349	0.0175	32.8503	0.02038	37.6871	0.0188	54.4442	0.01318
		2	86.5289	0.0054	94.0419	0.0085	100.127	0.0092	124.608	0.0091
		4	328.021	0.0014	335.851	0.00257	342.547	0.0030	372.404	0.0040

(2,2)	1	1	53.5933	0.00731	59.6525	0.01057	64.3118	0.01081	81.2693	0.009032
		2	132.746	0.0029	139.153	0.0049	144.445	0.0056	166.298	0.0062
		4	449.294	0.00088	455.885	0.0016	461.548	0.0019	487.053	0.00264
	4	1	41.2369	0.0112	48.3397	0.01516	53.7398	0.01498	73.6221	0.01197
		2	101.624	0.0046	109.197	0.0074	115.394	0.0082	140.74	0.0085
		4	343.111	0.00138	350.946	0.000247	357.653	0.0029	387.624	0.0038

3.2.1 Natural frequency of flat sandwich plate with ER core

In Fig. 3, the comparison diagram of the damping coefficient is shown in terms of vibrational modes and different electric fields.

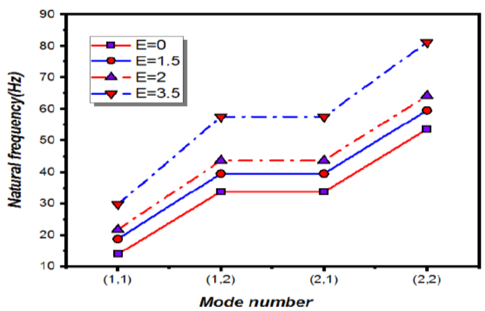

Fig.3
Diagram of changes in the natural frequency of the sheet, for different electric field intensities.

In general, it can be stated that the natural frequency grows with increasing electric field intensity due to a reduction in flexibility, where the modal damping coefficient decreases.

3.2.2 Influence of the ratio of core thickness to total sheet thickness on natural frequency

The core thickness has a very significant effect on the vibration of the sheet. Fig. 4 reveals the diagram of the first frequency changes of the flat sandwich plate with the ER core in terms of different core thickness to plate thickness (h_c/ h) ratios for different electric field intensities (KV/mm) at $a = b$.

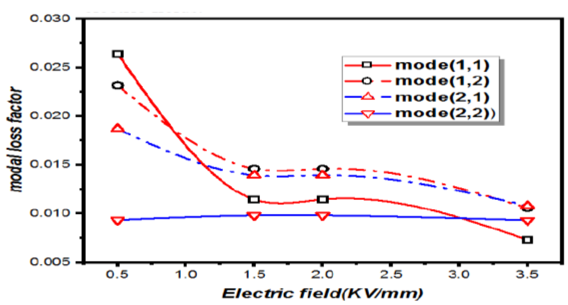

Fig.4
Diagram of changes in the damping coefficients in the first four vibrational modes, for different electric field intensities.

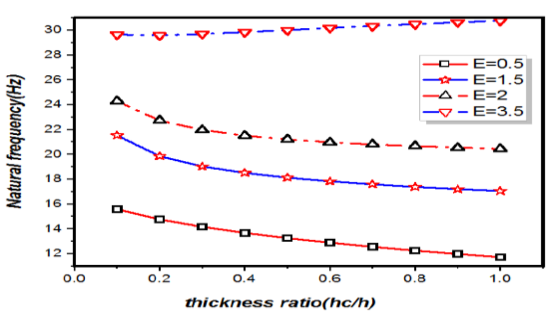

Fig.5
Diagram of the first frequency changes of the sheet in different ratios of core to sheet thickness, for different electric field intensities.

According to Fig. 5, it is observed that by increasing the ratio of core thickness to total sheet thickness, the natural frequency of the sheet diminishes. Since the core is made of oil and composite surfaces, the core modulus is smaller than the surfaces. Also, as the core thickness-to-whole ratio increases, the overall sheet modulus drops. As a result, the natural frequency of the sheet is also reduced. The oil density is also high and as the amount of oil increases, the sheet becomes significantly heavier and the stiffness-to-mass ratio falls, resulting in a decline in the natural frequency of the sheet.

3.2.3 Influence of fiber angle on natural frequency

Fig. 6 shows the diagram of the natural frequency changes of the first flat sandwich plate with the ER core in terms of the lay-up sequences for face sheets.

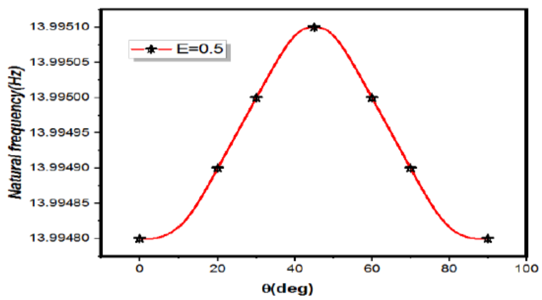

Fig.6
Diagram of the first frequency changes of the sheet in terms of the Chinese layer of the composite face sheets.

According to Fig. 6, it is observed that most of the natural frequency occurs in a state θ equal to 45 degrees. Because in this case the flexural stiffness has its maximum value.

3.2.4 Influence of electric field intensity on natural frequency

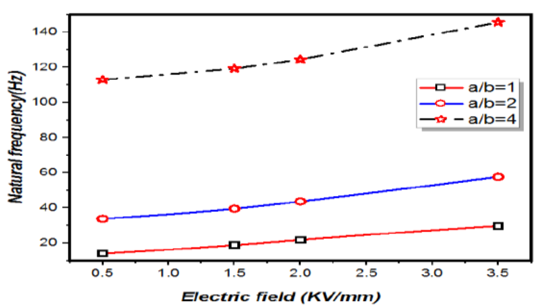

Fig.7
Diagram of the first frequency changes of the sheet in terms aspect Ratio for different electric field intensities.

According to Fig. 7, it is observed that as the electric field intensity increases, so does the natural frequency of the sheet. However, this increase in frequency only proceeds partly from the increase of the electric field intensity and does not increase from one value to the next, and is almost proved to be saturated as the intensity of the electric field, which in this study is approximately 3.5 kV/mm.

3.2.5 The effect of aspect ratio on natural frequency

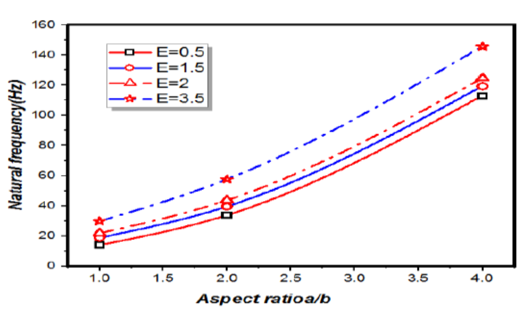

Fig.8
Diagram of the first frequency change of the sheet in terms of electric field intensity for different aspect ratio.

According to Fig. 8, it is observed that with increasing the aspect ratio, the natural frequency of the sheet increases. With the rise of the aspect ratio, the sheet gradually becomes a beam with enhanced transverse stiffness and thus augmented natural frequency. By raising the intensity of the electric field from one point to the next, its effect on the natural frequency increases. This is due to the saturation point; by increasing the intensity of the electric field, it saturates the oil at a given electric field intensity, after which increasing the field will not have much effect on increasing the rigidity and natural frequency of the sheet.

3.2.6 Influence of lenght-to-thickness ratio on natural frequency

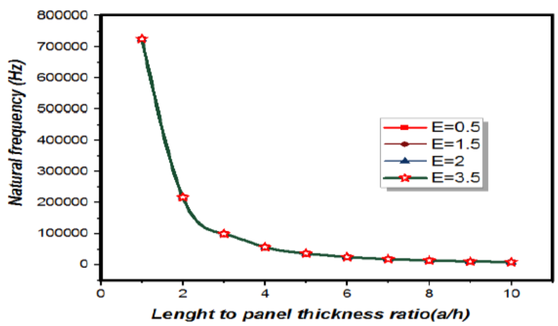

Fig.9
Influence of lenght-to-thickness ratio on natural frequency.

According to Fig. 9, it is observed that with increasing the length to thickness ratio, the natural frequency of the sheet decreases. As the ratio grows, the sheet becomes thinner and, as a result, its stiffness drops.

3.2.7 Flat sandwich plate displacement diagrams based on different mode shapes

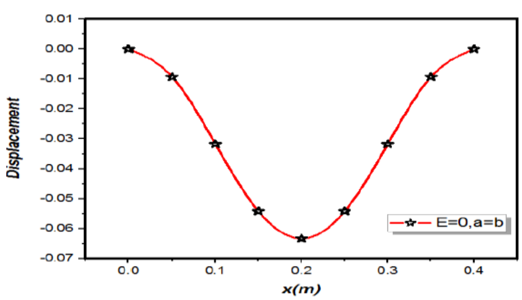

Fig.10
Displacement diagram of a flat sandwich plate based on the first mode shape.

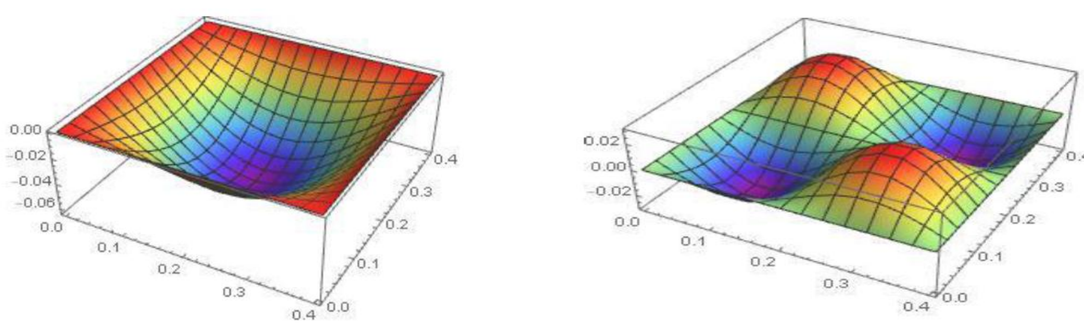

(a) First mode shape

(b) The fourth mode shape

Fig.11
Displacement diagram of a flat sandwich plate based on the a) first and b) fourth mode shape.

4 CONCLUSION

In this study, vibration of a sandwich plate with an ER fluid core, multi-layer face sheets, and four simply-supported edges were investigated. The Hamilton's solution method was used for the vibration analysis of sandwich structures. The generality of the problem indicates an increase in the natural frequencies of the sandwich plate for the ER state in the nucleus with increasing electric field intensity. However, this increase in frequency is only partially sustained by an increase in the intensity of the electric field and does not grow from one value to another and is almost constant. Thus, by creating an electric field whose intensity can be controlled, the natural frequencies and thus the vibrations of the structure can be controlled.

The effect of the thickness of the ER layer on the core is such that by increasing the ratio of the core thickness to the thickness of the whole sheet at a constant electric field intensity, a frequency drop is observed. Since the core is made of fluid and composite surfaces, the rigidity of the core is lower than that of the core, and as the core thickness-to-thickness ratio increases, the overall rigidity decreases. Also, as the fluid content rises, the sheet becomes significantly heavier and the stiffness to mass ratio diminishes. As the aspect Ratio increases, the sheet gradually becomes a beam whose transverse stiffness grows and thus the natural frequency increases. Thus, by altering this parameter, the natural frequency of the structure within the desired range can be obtained.

By increasing the length to thickness ratio, the natural frequency of the sheet decreases. As the ratio grows, the sheet becomes thinner and, as a result, its stiffness declines. Thus, by changing this parameter, the natural frequency of the structure can also be obtained within the desired range.

REFERENCES

[1] Yalcintas M., Dai H., 1999, Magnetorheological and electrorheological materials in adaptive structures and their performance comparison, *Smart Materials and Structures* **8**(5): 560-573.

[2] Hasheminejad S.M., Maleki M., 2009, Free vibration and forced harmonic response of an electrorheological fluid-filled sandwich plate, *Smart Materials and Structures* **18**(5): 16.

[3] Coulter J.P., 1993, Engineering application of electrorheological materials, *Journal of Intelligent Materials Systems and Structures* **4**(2): 248-259.

[4] Coulter J.P., Duclos T.G., 1989, Applications of electrorheological materials in vibration control electrorheological fluids, *2nd International Conference on Electro-Rheological Fluids ed Carlson J. D., Sprecher A. F., Conrad H., (Lancaster, PA: Technomic).*

[5] Coulter J.P., Duclos T.G., Acker D.U., 1989, The usage of electrorheological materials in viscoelastic layer damping applications , *WRDC-TR-89-3116* **1**: CAA-1.

[6] Yalcintas M., Coulter J.P., 1995, Analytical modeling of electrorheological material based adaptive beams, *Journal of Intelligent Material Systems and Structures* **6**(4): 488-497.

[7] Yalcintas M., Coulter J.P., 1995, Electrorheological material based adaptive beams subjected to various boundary conditions, *Journal of Intelligent Material Systems and Structures* **6**(5): 700-717.

[8] Yeh J.Y., Chen L.W., Wang C.C., 2004, Vibration of a sandwich plate with a constrained layer and electrorheological fluid core, *Composite Structures* **65**(2): 251-258.

[9] Yeh J.Y., Chen L.W., Wang C.C., 2007, Finite element dynamic analysis of orthotropic sandwich plates with an electrorheological fluid core layer, *Composite Structures* **78**(3): 368-376.

[10] Yeh J.Y., Chen L.W., Wang C.C., 2006, Dynamic stability analysis of a rectangular orthotropic sandwich plate with an ER fluid core, Composite Structures **72**(1): 33-41.

[11] Yeh J.Y., 2007, Vibration analyses of the annular plate with ER fluid damping treatment, *Finite Elements in Analysis and Design* **43**(11): 965-974.

[12] Yeh J.Y., Chen J.Y., Lin C.T., Liu C.Y., 2009, Damping and vibration analysis of polar orthotropic annular plates with ER treatment, *Journal of Sound and Vibration* **325**(1): 1-13.

[13] Yeh J.Y., 2011, Free vibration analysis of rotating polar orthotropic annular plate with ER damping treatment, *Composites Part B: Engineering* **42**(4): 781-788.

[14] Frostig Y., Thomsen O.T., 2004, Higher-order free vibration of sandwich panels with a flexible core, *International Journal of Solids and Structures* **41**(5): 1697-1724.

[15] Malekzadeh K., Khalili M.R., Mittal R.K., 2005, Local and global damped vibrations of plates with a viscoelastic soft flexible core: an improved high-order approach, *Journal of Sandwich Structures and Materials* **7**: 431-456.

[16] Reddy J.N., 1984, A simple higher-order theory for laminated composite plates, *Journal of Applied Mechanics* **51**(4): 745-752.

[17] Reddy J.N., 2004, *Mechanics of Laminated Composite Plates and Shells, Theory and Analysis*, CRC Press, New york.

[18] Ghugal Y.M., Sayyad A.S., 2011, Free vibration of thick orthotropic plates using trigonometric shear deformation theory, *Latin American Journal of Solids and Structures* **8**(3): 229-243.

[19] Belarbi M.O, Tati A., 2016, Bending analysis of composite sandwich plates with laminated face sheets: new finite element formulation, *Journal of Solid Mechanics* **8**(2): 280-299.
[20] Khorshidi K., Asgari T., Fallah A., 2015, Free vibrations analysis of functionally graded rectangular nano-plates based on nonlocal exponential shear deformation theory, *Mechanics of Advanced Composite Structures* **2**(2): 79-93.
[21] Bahrami M.R., Hatami A., 2016, Free and forced transverse vibration analysis of moderately thick orthotropic plates using spectral finite element method, *Journal of Solid Mechanics* **8**(4): 895-915.
[22] Mozaffari A., Karami M., Azarnia A.H., 2013, The effects of embedded SMA wires on free vibrations of shape memory sandwich-composite panel, *Aerospace Mechanics Journal* **44**(2): 29-40.
[23] Ghajar R., Malekzadeh K., Gholami M., 2015, Dynamic response analysis of doubly curved composite shells subjected to low velocity impact using two models of complete and improved spring-mass, *Aerospace Mechanics Journal* **10**(4): 1-12.
[24] Khorshidi K., Siahpush A., Fallah A., 2107, Electro-mechanical free vibrations analysis of composite rectangular piezoelectric nanoplate using modified shear deformation theories, *Journal of Science and Technology of Composites* **4**(2): 151-160.
[25] Ghorbanpour Arani A., Emdad M., Ashrafi H., Mohammadimehr M., Niknejad S., Ghorbanpour Arani A.A., Hosseinpour A., 2019, Analysis of viscoelastic functionally graded sandwich plates with CNT reinforced composite face sheets on viscoelastic foundation, *Journal of Solid Mechanics* **11**(4): 690-706.
[26] Carlson J.D., Coulter J.P., Duclos T.G.,1990, *Electrorheological Fluid Composite Structures*, 4,23,057 US Patent .
[27] Don D.L., 1993, *An Investigation of Electrorheological Material Adaptive Structures*, Master's Thesis, Lehigh University.
[28] Malekzadefard k., Malek-Mohammadi H., 2017, Free vibration and buckling analysis of Sandwich panels with flexible cores using an improved higher order theory, *Journal of Solid Mechanics* **9**(1): 39-53.
[29] Sun Q., Zhou J.X., Zhang L., 2003, An adaptive beam model and dynamic characteristics of magnetorheological materials, *Journal of Sound and Vibration* **261**(3): 465-481.
[30] Harland N.R., Mace B.R., Jones R.W., 2001, Adaptive-passive control of vibration transmission in beams using electro/magnetorheological fluid filled inserts, *IEEE Transactions on Control Systems Technology* **9**(2): 209-220.
[31] Ramkumar K., Ganesan N., 2009, Vibration and damping of composite sandwich box column with viscoelastic/electrorheological fluid core and performance comparison, *Materials and Design* **30**(8): 2981-2994.
[32] Rajamohan V., Sedaghati R., Rakheja S., 2010, Vibration analysis of a multi-layer beam containing magnetorheological fluid, *Smart Materials and Structures* **19**(1): 1-12.
[33] Rajamohan V., Rakheja S., Sedaghati R., 2010, Vibration analysis of a partially treated multi-layer beam with magnetorheological fluid, *Journal of Sound and Vibration* **329**(17): 3451-3469.
[34] Rajamohan V., Sedaghati R., Rakheja S., 2010, Optimum design of a multilayer beam partially treated with magnetorheological fluid, *Smart Materials and Structures* **19**(6): 58-73.
[35] Payganeh G., Malekzadeh K., Malek-Mohammadi H., 2016, Free vibration of sandwich panels with smart magneto-rheological layers and flexible cores, *Journal of Solid Mechanics* **8**(1): 12-30.
[36] Malekzadeh k., Livani M., Ashenai Ghasemi F., 2014, Improved high order free vibration analysis of thick double curved sandwich panels with transversely flexible cores, *Latin American Journal of Solids and Structures* **11**(12):2284-2307.
[37] Reddy J.N.,1987, A refined nonlinear theory of plates with transverse shear deformation, *Journal of Solids and Structures* **20**(9): 881-896.
[38] Vinson J.R., 1986, Optimum design of composite honeycomb sandwich panels subject to uniaxial compression, *AIAA Journal* **24**(10): 1690-1696.
[39] Sanders J.R., Lyell J.,1959, *An Improved First Approximation Theory for Thin Shells*, NASA THR24.
[40] Lall A.K., Asnani N.,T., Nakra B.C., 1987, Vibration and damping analysis of rectangular plate with partially covered constrained viscoelastic layer, *Journal of Vibration, Acoustics, Stress, and Reliability in Design* **109**(3): 241-247.